Climate Dynamics
https://doi.org/10.1007/s00382-021-05712-0

Simulation of interannual relationship between the Atlantic zonal mode and Indian summer monsoon in CFSv2

Vijay Pottapinjara[1] · Mathew Koll Roxy[2] · M. S. Girishkumar[1] · Karumuri Ashok[3] · Sudheer Joseph[1] · M. Ravichandran[1,4] · R. Murtugudde[5]

Received: 17 July 2020 / Accepted: 2 March 2021

Abstract
Recent studies have shown that the Atlantic zonal mode (AZM) can significantly influence the Indian summer monsoon (ISM). In an earlier study, we proposed that AZM influence propagates in tropospheric temperature as Kelvin wave-like features to the east to reach the Indian Ocean and influences the monsoon by modulating the mid-tropospheric land-sea thermal gradient and thereby the seasonal mean flow. The changes thus induced in the mean flow were shown to affect the monsoon depressions in the Bay of Bengal and rainfall over India. In the present study, we use the Coupled Forecast System version 2, which is utilized for seasonal prediction of ISM in India, to examine how well the model simulates this AZM-monsoon link. In the sensitivity experiment, a warm AZM SST anomaly is added over the tropical Atlantic in the boreal summer and the ISM response is studied. We find that the model simulates the important aspects of the AZM-monsoon link. The model also simulates a known dynamics-based mechanism wherein a warm AZM SST anomaly produces a Matsuno-Gill type response, which in turn induces a sinking motion over India causing a reduction in rainfall. However, some finer details of these mechanisms are not simulated due to mean state biases in the tropical Atlantic in the model, a problem common to many coupled models. Our study highlights the need for the improvement of mean state of model in the tropical Atlantic to better capture the AZM-ISM relationship which will ultimately improve the monsoon forecasts issued using this model.

Keywords Tropical Atlantic · Indian summer monsoon · Interannual variability · Teleconnection · CFSv2 · Coupled model biases

1 Introduction

The livelihood and well-being of people living in India and surrounding countries depend, to a great extent, on the Indian monsoon during summer. The Indian summer monsoon Rainfall (ISMR) exhibits variability on diurnal to decadal and longer timescales (e.g., Sikka 1980; Parthasarathy et al. 1994; Webster et al. 1998; Krishnamurthy and Shukla 2000; Gadgil 2018). Although the interannual variability of the ISMR is only about 10% of the mean (long term mean is 850 mm; e.g., Kothawale and Rajeevan 2017), these year-to-year variations of ISMR have a significant impact on the food production and economy of the region which is home to millions of people (e.g., Gadgil and Gadgil 2006; Amat and Ashok 2018). Hence, it is important to understand what contributes to the interannual variability of the ISMR, especially during the non-ENSO years, and anticipate its variations well in advance to prepare for any possible disasters like floods and droughts.

Interannual variability of the monsoon is a result of an interplay of both the internal dynamics of the monsoon and the slowly varying external forcings such as El Niño-Southern Oscillation (ENSO; e.g., Rasmusson and Carpenter 1982; Philander 1989). The influence of these external factors on the monsoon forms the predictable part of the

✉ Vijay Pottapinjara
vijay.p@incois.gov.in

[1] Indian National Centre for Ocean Information Services, Ministry of Earth Sciences, Hyderabad, India

[2] Indian Institute of Tropical Meteorology, Ministry of Earth Sciences, Pune, India

[3] Centre for Earth, Ocean and Atmospheric Sciences, University of Hyderabad, Hyderabad, India

[4] National Centre for Polar and Ocean Research, Ministry of Earth Sciences, Goa, India

[5] Earth System Science Interdisciplinary Center, University of Maryland, College Park, MD, USA

Published online: 29 March 2021

monsoon variability (e.g., Keshavamurty 1982; Mooley and Parthasarathy 1984; Gadgil and Sajani 1998; Webster et al. 1998; Ashok et al. 2019 and references therein). Recent advances have highlighted the influences of the strong positive Indian Ocean Dipole events (IOD; also referred to as Indian Ocean zonal mode; Saji et al. 1999; Webster et al. 1999; Behera et al. 1999; Murtugudde et al. 2000; Ashok et al. 2001) as well.

Earlier studies suggest that the tropical Atlantic also hosts a mode of interannual variability called the Atlantic zonal mode (AZM) or the Atlantic Niño which is similar to, but weaker than, ENSO (e.g., Zebiak 1993; Ruiz-Barradas et al. 2000; Servain et al. 2000; Lübbecke et al. 2018 and references therein). It peaks in boreal summer (June–August; e.g., Zebiak 1993), and its life cycle is also shorter compared to ENSO: an AZM lasts for 3–4 months whereas an ENSO event generally lasts for 6–24 months (Lübbecke and McPhaden 2013). The studies on the effect of the AZM on monsoon are still limited but have started to gain attention recently (Kucharski et al. 2008, 2009, 2016; Wang et al. 2009; Barimalala et al. 2013; Pottapinjara et al. 2014, 2016; Yadav et al. 2018; Sabeerali et al. 2019a, b; Pottapinjara 2020). In the following, we will briefly discuss some of the studies that are most relevant for our current study.

A series of studies by Kucharski et al. (2007, 2008, 2009) based on the analysis of observational/reanalysis datasets and sensitivity experiments conducted using an Atmospheric General Circulation Model (AGCM), shows the existence of a relation between AZM and ISMR in which a warm (cold) AZM event leads to a low-level divergence (convergence) over India and thereby reduced (enhanced) ISMR. In Pottapinjara et al. (2014), we have shown that the AZM also affects the monsoon transients: in response to a warm (cold) AZM event, the number of monsoon depressions forming in the Bay of Bengal (BoB) decreases (increases) and thereby contributes to a reduction (an enhancement) of rainfall over India. Also, we have proposed a physical mechanism in which the AZM influence propagates in tropospheric temperature via Kelvin wave-like features to the east to reach the Indian Ocean and influences the Indian monsoon by modulating the mid-tropospheric land-sea thermal gradient and thereby the seasonal mean flow (Pottapinjara et al. 2014). This mechanism involves a thermodynamic aspect of the teleconnection between the AZM and ISM. The changes thus induced in the mean flow were shown to affect the monsoon depressions in the BoB and rainfall over India (detailed discussion in Sect. 3.2). Further, in Pottapinjara et al. (2016) we discussed the possible predictors such as heat content which can foretell the development of an AZM event and thereby the impact on the monsoon, one season in advance.

For optimum societal benefit, process understanding of the monsoon variability, and the efforts to forecast it must go hand in hand. The India Meteorological Department (IMD) is the agency tasked with the responsibility of providing meteorological services including the monsoon forecasts, in India. Currently, the IMD uses a suite of statistical (Pai et al. 2011; Kumar et al. 2012) and dynamical (Pai et al. 2017, 2019) models to forecast the monsoon. In addition to these existing models, the IMD has recently adopted a variant of the Coupled Forecasting System version 2 (CFSv2; Saha et al. 2014a) for the operational monsoon forecasts (Ramu et al. 2016; Sahai et al. 2019; Pattanaik et al. 2019; Pai et al. 2019; Rao et al. 2019). CFSv2 is a state-of-the-art coupled ocean–atmosphere general circulation model, originally developed by the National Centers for Environmental Prediction (NCEP).

Earlier studies have shown that the CFSv2 simulates the general features of the monsoon such as the onset, withdrawal, seasonal mean patterns of spatial rainfall distribution and wind circulation, and the variability of monsoon reasonably well (e.g., Jiang et al. 2013; Saha et al. 2014a,b). However, it has some serious biases, especially, a dry bias over land and cold SST bias over the Indian Ocean (Saha et al. 2014b; Narapusetty et al. 2016, 2018; Sahana et al. 2019). The model captures the warmer tropospheric temperatures over Tibetan Plateau compared to those over the Indian Ocean but it underestimates the mean tropospheric temperature and tropospheric temperature gradient between the land and ocean (Saha et al. 2014a, b). The ISM in the model is rightly phase locked to the boreal summer (June–September) but the onset is delayed by about 7 days in the model (Saha et al 2014a, b). The success of monsoon forecasts using the CFSv2 depends on, among other things, how well the model simulates the links of the monsoon with external factors. Previous studies have investigated the simulation of ENSO and IOD, and their relation to the ISMR in the model (e.g., George et al. 2016; Saha et al. 2016; Shukla and Huang 2016; Krishnamurthy 2018) and report that while the ENSO-monsoon relation is too strong compared to observations probably because of the deficiencies associated with the simulation of ENSO in the model, the IOD-monsoon relation is completely out of phase due to inadequate representation of coupled dynamics over the Indian Ocean. However, the simulation of AZM and its relation to the ISMR in the model are yet to receive their due attention. In a recent study, Sabeerali et al. (2019b) analyze the hindcasts of CFSv2 initialized in two months (February and May) and show that the simulation that erroneously forecasts the AZM (initialized in February) loses predictive skill for the monsoon. They also show that although the hindcasts initialized in May improve on prediction skill for the AZM, the misrepresentation of ENSO-ISMR relationship in the May-initialized hindcasts leads to a lower skill for the ISMR compared to the February-initialized hindcasts. Further, they demonstrate an improvement in the prediction skill for the ISMR by combining the ISMR induced by

ENSO and AZM in hindcasts initialized in February and May, respectively. While their interest was on assessing the predictive skill of the AZM in the model, in this study, we will focus more on the simulation of observed AZM-ISM relation and teleconnections in the model, particularly as proposed in our recent study (Pottapinjara et al. 2014). We attempt to achieve this goal by analyzing the AZM-ISM relationship in the free-run simulations of the model and by conducting a sensitivity experiment which can be expected to show the cause-and-effect in the AZM-ISM relationship more clearly. This helps in identifying the shortcomings, if any, in the model with respect to AZM-ISM relation and should potentially contribute to improving the forecasts of ISM issued using this model.

In the next section, we will describe the datasets used and general methodology, the CFSv2 model, and the model experiments we carried out. In Sect. 3, we will at first examine the representation of the mean state in the tropical Atlantic (Sect. 3.1) and the simulation of the AZM and its relation to ISMR in a free-run or reference run we carried out with the model (Sect. 3.2). Further, in Sect. 3.3, we will present the details of a complementary sensitivity experiment in which the SST anomaly associated with the AZM in the tropical Atlantic is imposed, and the response of ISM to that anomaly is examined. The final Sect. 4 presents a summary of results, followed by a discussion.

2 Observations and model simulations

2.1 Observational data and methods

The Hadley Centre Sea Ice and Sea Surface Temperature (HadISST; Rayner et al. 2003) is used for the model sensitivity experiment (see Sect. 2.4 for details). The AZM variability in this study is represented by the Atl3 index which is the area-average of SST anomalies in the Atl3 region (3° S – 3° N and 20° W – 0° E; Zebiak 1993; Burls et al. 2012). A warm (cold) AZM event is considered to occur whenever the June–August (JJA) Atl3 index exceeds (falls below) the + 1 (−1) of its standard deviation. The Oceanic Niño Index (ONI) which is the average of SST anomalies in Niño 3.4 region (5° S – 5° N and 170° W – 120° W) is used as an index of ENSO. The monthly precipitation data from the Global Precipitation Climatology Project (GPCP; Adler et al. 2003) is also used. The meridional position of the Atlantic ITCZ is identified as the latitude at which the meridional component of the surface winds vanishes along 28°W between the latitudes of 5° S and 20° N (Servain et al. 1999; Pottapinjara et al. 2019). The wind data from the European Centre for Medium-Range Weather Forecasting (ECMWF)'s Reanalysis, known as the ERA-Interim (Dee et al. 2011) is used to validate the model performance. The Tropospheric Temperature (TT) data is also taken from ERA-Interim reanalysis. The observational analyses presented in this study are based on the data for a common period of 1979–2012 unless mentioned otherwise.

As discussed already in the Introduction, ENSO impacts ISM at interannual timescales. Earlier studies suggest that ENSO also affects AZM, with an El Niño (La Niña) event during boreal summer accompanying a cold (warm) AZM event (e.g., Kucharski et al. 2009; Wang et al. 2009; Pottapinjara et al. 2014). To show the direct relationship between the AZM and ISM in the analysis clearly, we have regressed out the effect of ENSO on a target field (Kucharski et al. 2008; Pottapinjara et al. 2016), whenever necessary. Regressing out the impact of ENSO involves a subtraction of the product of ENSO index (ONI) time series, and the linear regression slope between ENSO and the target field from the target field time series. The resultant (ENSO-influence-free) time series of the target field is used in further analysis. Whenever the ENSO influence is regressed out, it is explicitly mentioned while discussing the respective analysis. However, it must be noted that this method cannot remove the effect of ENSO completely. The Student's *t* test is used to determine the level of significance of relevant statistics. In the following, the season boreal spring refers to the months of March–May and boreal summer refers to the period June–September unless mentioned otherwise.

2.2 The model

In this study, we use one of the configurations of the NCEP-CFSv2 model being utilized at the Indian Institute of Tropical Meteorology, India (Saha et al. 2014a, b). The atmospheric component of the model has a resolution of T126 (0.9°) in the horizontal and has 64 sigma-pressure hybrid levels in the vertical. The oceanic component has a horizontal resolution of 0.25° – 0.5° and 40 vertical levels. The ocean–atmosphere coupling information is exchanged every 0.5 hours. A variant of this model is used in operational seasonal forecasting and is successful in representing the key monsoon processes (e.g., Roxy et al. 2015).

2.3 Model reference run

In our simulations, we use a 100-year free-run of the CFSv2 coupled model (also referred to as the reference run or $CFSv2_{REF}$) starting with the well-balanced ocean and atmospheric initial conditions. The reference run ($CFSv2_{REF}$) includes a constant external forcing in terms of mixing ratios of, for instance, the atmospheric CO_2, N_2O, and CH_4, of the present-day values. With the appropriate initial and boundary conditions, this ensures that the model climate is comparable with the observed climate of the recent decades (Saha et al. 2014a, b; Roxy et al. 2013, 2015). The performance

of the model in simulating the systems involved in AZM-ISM links is diagnosed using 40 years of the model free-run or $CFSv2_{REF}$, leaving the first 50 years of the free-run for allowing the model to reach a dynamical stability. From the results of the analysis presented in Sect. 3, it will be shown that the model simulates seasonal cycle of the tropical Atlantic, and the AZM and its relation with the ISM reasonably well, despite some mean state biases.

Apart from examining whether or not the model simulates the observed AZM-ISM relationship, it is also our goal to validate if the physical mechanism we proposed in Pottapinjara et al. (2014) is indeed at work. However, the influence of AZM on ISM and the physical mechanism cannot be delineated from the analysis presented in Sect. 3.1 using $CFSv2_{REF}$ alone. With the flexibility of conducting sensitivity experiments, the model comes in handy to test if the AZM in fact affects the ISM the way we see it in the observations. The difference between the reference and sensitivity runs tells us the effect of AZM anomalies on ISM, in other words, the cause-and-effect becomes clearer. Therefore, the model is used to conduct a sensitivity experiment to see how the ISM responds to an imposed SST anomaly associated with the observed warm AZM events. The details of how the imposed SST anomaly is constructed is discussed later.

2.4 Model sensitivity experiment

The sensitivity experiment (referred to as the $CFSv2_{SST}$ hereafter) is similar to Roxy et al. (2015) and is designed as follows. We start from the model state in the month of May of every year of a 20-year period of the 40-year free-run ($CFSv2_{REF}$) and impose the SST anomaly pattern associated with the observed warm AZM events in the tropical Atlantic (presented in Sect. 3.2) from June through September of each year. These are the months when both the AZM and ISM occur, as they are seasonally phase locked to this period. The atmospheric component of the coupled model responds, to the combined SSTs (SST produced by the ocean component + observed AZM SST anomaly pattern added at the coupler level) in the tropical Atlantic, and to SSTs coming from the oceanic component everywhere else. In simpler words, the $CFSv2_{SST}$ differs from the $CFSv2_{REF}$ by having an additional warm AZM-like SST anomaly in the tropical Atlantic at the coupler level. Thus, the model is coupled everywhere in its domain. The experiment ($CFSv2_{SST}$) comprises 20 runs, each lasting only for the June–September season of every year of the 20-year period. Note, however, that the SST anomaly pattern imposed in the tropical Atlantic in $CFSv2_{SST}$ runs, is kept the same throughout the experiment period to keep the experiment simple. Thus, this ensemble of runs with different initial states (all taken from $CFSv2_{REF}$ in the respective years of the 20-year period) but with the same imposed boreal summer SST anomaly in the tropical Atlantic, constitutes the sensitivity experiment ($CFSv2_{SST}$). The average of differences between the sensitivity run ($CFSv2_{SST}$) and the reference run ($CFSv2_{REF}$), i.e., the average of $CFSv2_{SST}-CFSv2_{REF}$ over the common period, represents the response of the model to the imposed SST anomaly (Figs. 9, 10, 11, 12, 13). It may be noted that while Roxy et al. (2015) impose an SST trend in the western Indian Ocean to study the associated climate change impact on the ISM, we impose the AZM SST anomaly pattern in the tropical Atlantic to understand AZM-monsoon links.

As discussed above, the observed warm AZM SST anomalies in the tropical Atlantic are added to the surface temperature or SST from the ocean at the coupler level before passing them onto the atmospheric model. Since these SST anomalies are not added directly to the ocean model in the tropical Atlantic, it is not meaningful to explore the ocean conditions in the tropical Atlantic. However, it may be relevant to explore resultant SSTs passed to the atmosphere in the tropical Atlantic to gain insights.

The SST anomaly added at the coupler level every summer on the simulated SST in the tropical Atlantic is prepared from the observed SST data in the tropical Atlantic, as follows: (1) monthly SST anomalies (SSTA) are averaged over the period of June–August (JJA) of each year during 1950–2012, (2) JJA SSTA are de-trended, and (3) the de-trended anomalies are composited in all those years when there is a warm AZM event during the period. Note that this pattern is composited over June–July–August but in the sensitivity experiment, it is kept imposed throughout June–July–August–September as described earlier. As the cold tongue, the interannual modulation of which manifests as the AZM (Burls et al. 2012; Lübbecke et al. 2018), develops late in the model ($CFSv2_{REF}$) by one or two months (see Sect. 3.1), the season over which the sensitivity experiment conducted is extended by one month, i.e., into September. Also, ISM, whose relationship with AZM is the focus of this study, is still active in September.

It is possible to design the sensitivity experiment alternatively and more sophisticatedly. For instance, the imposition of an AZM pattern which varies within the experiment season may be more realistic but the present design is adapted for the sake of simplicity. Alternatively, an AZM anomaly pattern derived from the reference run ($CFSv2_{REF}$) itself multiplied by an ad hoc factor to address the weak amplitude of AZM in the model (see Sect. 3.2), can be imposed. However, this approach does not address the issue of the narrow spatial extent of model simulated AZM compared to that of observations (Sect. 3.2). Nevertheless, despite being simplistic, our present experiment design reproduces the observed AZM-ISM relationship adequately (see Sect.3.3).

3 Results and discussion

3.1 Mean state of the tropical Atlantic in CFSv2 reference run

Before examining how the model simulates the relationship between the AZM and ISM, it is imperative to see if the model simulates the climatological features in the two ocean basins, i.e., tropical Atlantic and Indian Oceans. As discussed already in the Introduction, earlier studies have shown that the CFSv2 simulates the climatological features of ISM including the tropospheric temperature gradient between the land and ocean, and the interannual variability of ISM faithfully despite some mean state biases (e.g., Jiang et al. 2013; Saha et al. 2014a,b, 2016; Narapusetty et al. 2016, 2018; George et al. 2016; Shukla and Huang 2016; Krishnamurthy 2018; Sahana et al. 2019). Therefore, we will not analyze the simulation of the mean ISM or its variability in this study but will focus on the simulation of the seasonal cycle in the tropical Atlantic in the following analysis.

The observed monthly climatological evolution of SST and surface winds in the tropical Atlantic is shown in Fig. 1. The band of high SSTs with temperatures above 25 °C migrates in the north–south direction with the season.

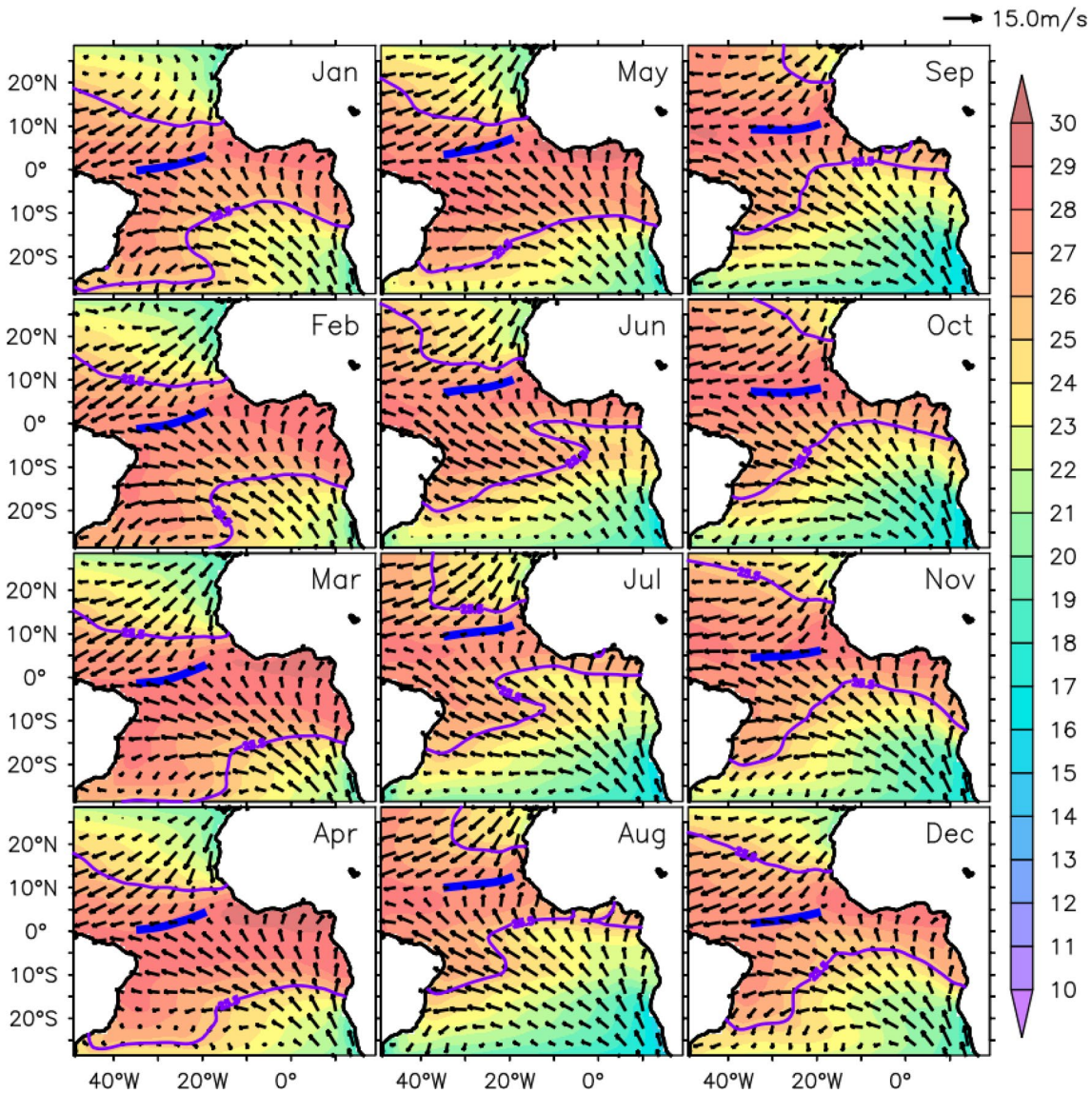

Fig. 1 Observed monthly climatology of SST (°C; shaded) overlaid by surface winds (vectors), and position of the oceanic ITCZ (thick blue line) in the tropical Atlantic. The SST contour of 25.5 °C is overlaid (blue) to show the development of the seasonal cold tongue in the southern tropical Atlantic during boreal spring–summer. The corresponding month is indicated on each subpanel

Notably, it is followed by a zone of convergence of the trade winds from either hemisphere, i.e., the Inter-tropical Convergence Zone (ITCZ) with a delay of about one month. With the progress of the season, and as a result of intensified winds and northward excursion of the ITCZ during late boreal spring to early boreal summer, i.e., March–June, the thermocline in the southeastern Atlantic shoals. The associated upwelling leads to a drop of about 5 °C in SST and thereby leads to the development of a distinctive seasonal cold SST tongue with temperatures below 25 °C in the eastern equatorial Atlantic during boreal summer (Fig. 1; Dippe et al. 2018). The cold tongue region has the highest SST variability, and the interannual modulation of the cold tongue in terms of its timing of occurrence and/or strength manifests as an AZM event (e.g., Burls et al. 2012; Lübbecke et al. 2018).

The bias of the model in simulating the seasonal cycle of SST and surface winds in the Atlantic is shown in Fig. 2. It

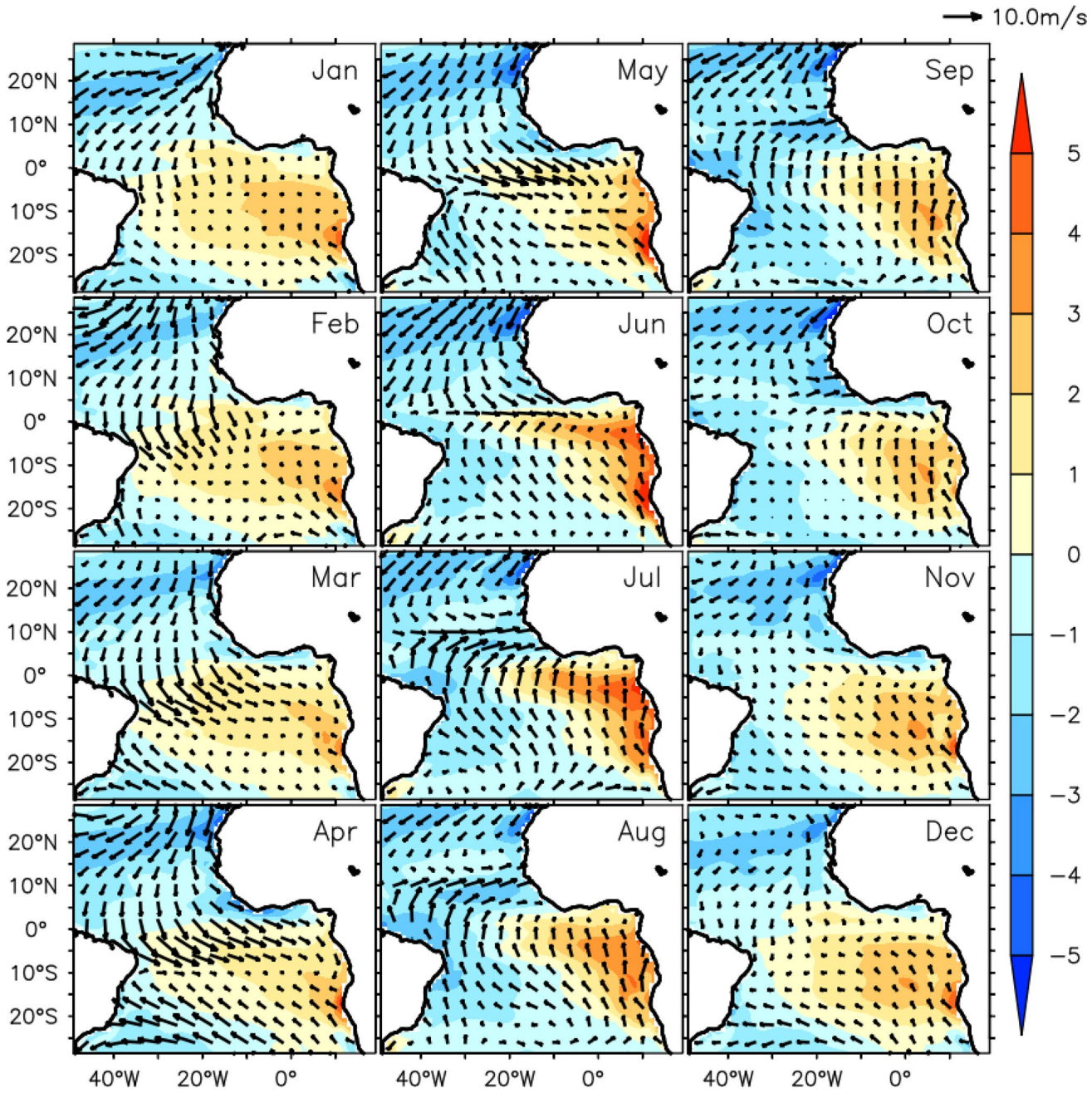

Fig. 2 Monthly evolution of the bias ($CFSv2_{REF}$ − Observations) in SST (shaded; °C) and surface winds (vectors; ms^{-1}) when the reference run is compared against observations

can be seen from the figure that there is a warm SST bias in the equatorial and tropical south Atlantic throughout the year. A strong warm bias of about 3 °C in the equatorial and tropical south Atlantic can be also observed during May–September, and it has the highest spatial extent in June–July. The winds over the equatorial Atlantic have a northwesterly bias during January–June and a southwesterly bias during July–December. Irrespective of the direction, the equatorial Atlantic wind bias is the highest with a magnitude of about 6 ms^{-1} in April–May. Particularly, the zonal winds in the equatorial Atlantic have a westerly bias throughout the year and this bias is the highest during boreal spring. The warm SST bias in the southeastern tropical Atlantic follows that of equatorial Atlantic zonal winds with a delay of about 2 months, during boreal spring–summer. Note that the model bias in SST in summer has a structure similar to that of the seasonal cold tongue shown in Fig. 1. These biases are essentially consistent with the well-known biases in other coupled climate models (Richter et al. 2014; Richter and Tokinaga 2020).

Simulation of the development of seasonal cold tongue in the tropical Atlantic is important for the model to capture the AZM properly, although a few coupled models can reproduce interannual variability despite mean state biases (Richter and Tokinaga 2020). As seen in the observations (Fig. 1), the meridional movement of ITCZ is strongly tied to the seasonal cycle (e.g., Xie and Carton 2004; Lübbecke et al. 2018) and examining the climatological meridional movement of ITCZ in the tropical Atlantic in the model may reveal more about the SST bias. A comparison of the monthly climatological meridional position of the Atlantic ITCZ along 28°W in the model reference run with that of the observations is shown in Fig. 3. General observed features of the Atlantic ITCZ spending most of its time (about 8 months in a year) in the northern hemisphere, and occupying the southernmost position in boreal spring and the northernmost position in boreal summer are captured accurately by the model along with its seasonal migration (in $CFSv2_{REF}$). However, the Atlantic ITCZ in the model is not collocated with that of the observed most of the year. The model Atlantic ITCZ is the farthest from the observed ITCZ during boreal spring by 3–5 degree latitude, with the model ITCZ to the south of the observed ITCZ, but the difference between their meridional positions reduces in the later months leading up to midsummer. Hence, the model ITCZ (in $CFSv2_{REF}$) lags behind the observed ITCZ by 1–2 months during spring to early summer. It all reflects the delayed Atlantic seasonal cycle during the spring to summer transition in the model.

Because of the further southward location of the model ITCZ (in $CFSv2_{REF}$) compared to the observed during spring (Fig. 3), the southeast trades are weak which explains the northwesterly/westerly surface wind bias over the equator in the model (Fig. 2). As a result, the development of the cold tongue is delayed which causes the warm SST bias during late spring to summer as shown in Fig. 2. These biases

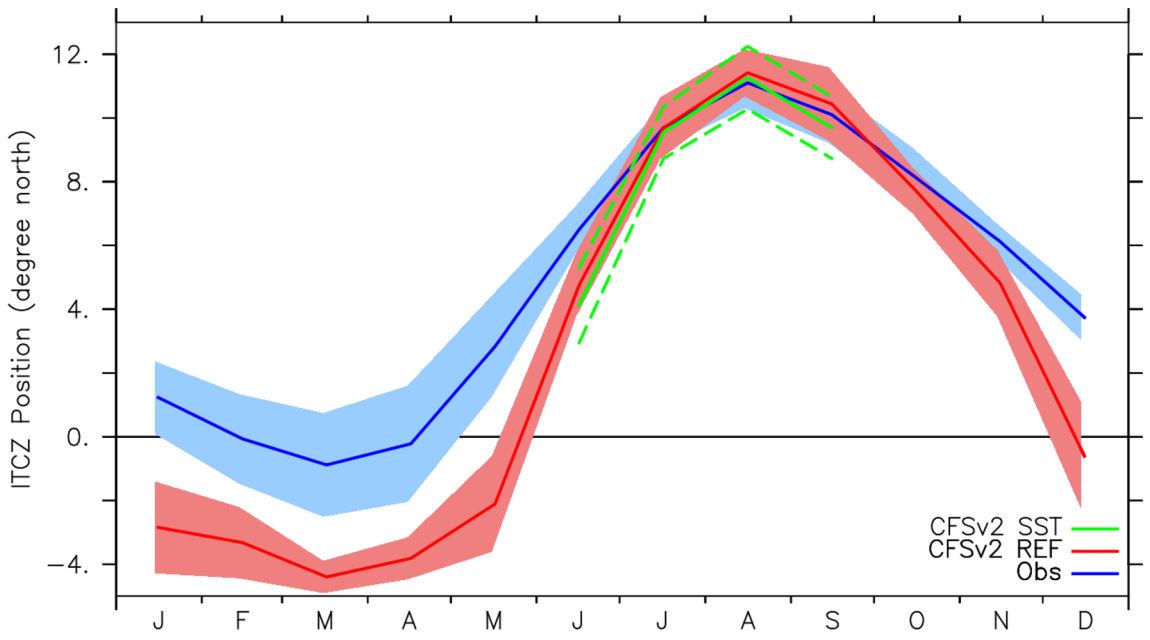

Fig. 3 Monthly climatological position of the ITCZ (degree north) in the Atlantic in the model reference run ($CFSv2_{REF}$; red) and in observations (blue) with the shading indicating the standard deviation about the mean position of ITCZ in the respective months. The mean position of the Atlantic ITCZ in the model sensitivity experiment ($CFSv2_{SST}$; light green) during June–September is overlaid, with the dashed lines in light green indicating the standard deviation about its mean position

in SST in the cold tongue region, surface winds over the equator, and the meridional position of ITCZ are all intimately connected with each other and the biases decrease after July. It should be noted that the position of the ITCZ in the model almost coincides with the observed one in mid-to-late boreal summer (July–September; Fig. 3). As we will see later, this point becomes important when interpreting the results of the sensitivity experiment discussed in Sect. 3.3. From the above, we can conclude that the model simulates the important climatological features in the tropical Atlantic such as the development of characteristic seasonal cold tongue although with a delay of one or two months during spring to summer which gives rise to the warm SST bias during late spring to summer. As stated earlier, the warm SST bias in the southeastern tropical Atlantic is a major problem plaguing many models participating in the Coupled Model Intercomparison Project 5 (CMIP5) and the earlier studies attribute this bias to drawbacks in the proper simulation of physics of ocean and atmosphere, and insufficient model resolution of the atmospheric and oceanic components (e.g., Xu et al. 2014; Richter 2015; Zuidema 2016; Harlaß et al. 2018; Cabos et al. 2019; Goubanova et al. 2019). Particularly, Richter (2015) points out that the SST bias is likely caused by errors in surface winds in the equatorial Atlantic and winds alongshore the coast of Angola. The errors in the simulation of winds in the equatorial Atlantic exert a remote influence on the upwelling along the coast of Angola via oceanic Kelvin waves. The curl of alongshore winds directly control the local upwelling. He also highlights that meso-scale eddies play an important role in offshore oceanic transport in the southeastern tropical Atlantic and a coarse resolution model such as CFSv2 used in this study may not sufficiently resolve these eddies, thus contributing to the SST bias (e.g., Marchesiello et al. 2003; Colas et al. 2012; Goubanova et al. 2019).

From earlier studies, we know that the interannual SST anomaly of the cold tongue, and its accompanying anomalous winds and the thermocline depth, among other things, manifest as an AZM event (Zebiak 1993; Xie and Carton 2004; Lübbecke et al. 2018). Having shown that the model simulates the development of seasonal cold tongue in the tropical Atlantic, we examine below how well the model simulates the AZM using a free-run ($CFSv2_{REF}$) of the model.

3.2 Simulation of the AZM and its links with the ISM in CFSv2 reference run

The composites of anomalies of SST and winds of cold and warm AZM events (see Sect. 2.1 for the identification of events) in the CFSv2 free-run (or $CFSv2_{REF}$) are compared with that of the observations in Fig. 4. In the observations, the SST anomalies associated with an AZM event peak in June–July and decay thereafter. These SST anomalies extend from the coast of Angola to the Atl3 region (3°S–3°N and 20°W–0°E) over the equator (Fig. 4a) and are accompanied by divergent (convergent) surface winds during a cold (warm) event. The northerly (southerly) wind anomalies along the Angolan coast in the latter months of July and August, among other things, contribute to the decay of a cold (warm) event (Fig. 4a; e.g., Zebiak 1993; Jansen et al. 2009). In the model, the timings of the peak and decay of AZM events are captured very well (Fig. 4b). However, the magnitude and spatial extent of simulated AZM SST anomalies are weaker compared to that in observations (compare Fig. 4a , b). Further, these SST anomalies are restricted mostly to an area between 10° S and 5° N and are less well connected to those off the coast of Angola (Fig. 4b), when compared to observations. As discussed earlier in Sect. 3.1, various processes influence the simulation of SST in the southeastern tropical Atlantic (e.g., Xu et al. 2014; Richter 2015; Cabos et al. 2019) and an erroneous simulation of the contributing processes in the model can dictate the strength and spatial extent of the interannual AZM SST anomalies. For instance, the upwelling and the SSTs off the coast of Angola, are controlled largely by the local winds off Angola and remote winds in the western equatorial Atlantic. Unless the model simulates all the contributing processes well, the model simulated SST and its interannual variability can not be realistically simulated. Missing meso-scale eddies in the low resolution CFSv2 can also contribute to the deficiencies of AZM since a coupled model can extend coastal influences into the tropics. Model deficiencies in simulating the coastal processes and the cascade of those biases into large-scale coupled climate variability have been an issue for well over a decade (Large and Danabasoglu 2006). However, we will not go into those details in this study as that is not our focus. Nonetheless, the important feature of the phase locking of AZM to the seasonal cycle is captured by the model (Fig. 4). Examining the interannual variability of the AZM in the model, the simulated standard deviation of the JJA Atl3 index is 0.31 against the observed value of 0.48 implying that the simulated variability of AZM is weaker in the model ($CFSv2_{REF}$) compared to observations during June–August (Fig. 5). It is worth noting that the standard deviation of JJA Atl3 index in the $CFSv2_{REF}$ of 0.31 is also lower than that of most other CMIP5 models which is 0.5 (Richter et al. 2014). Although the AZM in the model is weak and less variable compared to observations, it can be concluded that the model simulation of the AZM is quite adequate for our goal here.

The relationship between AZM and ENSO in $CFSv2_{REF}$ (free-run) is briefly discussed here. The correlation between JJA Atl3 and JJA ONI in the model is 0.21 in contrast to − 0.41 in observations. While the AZM and ENSO have an opposite phase relation in the observations (e.g., Kucharski

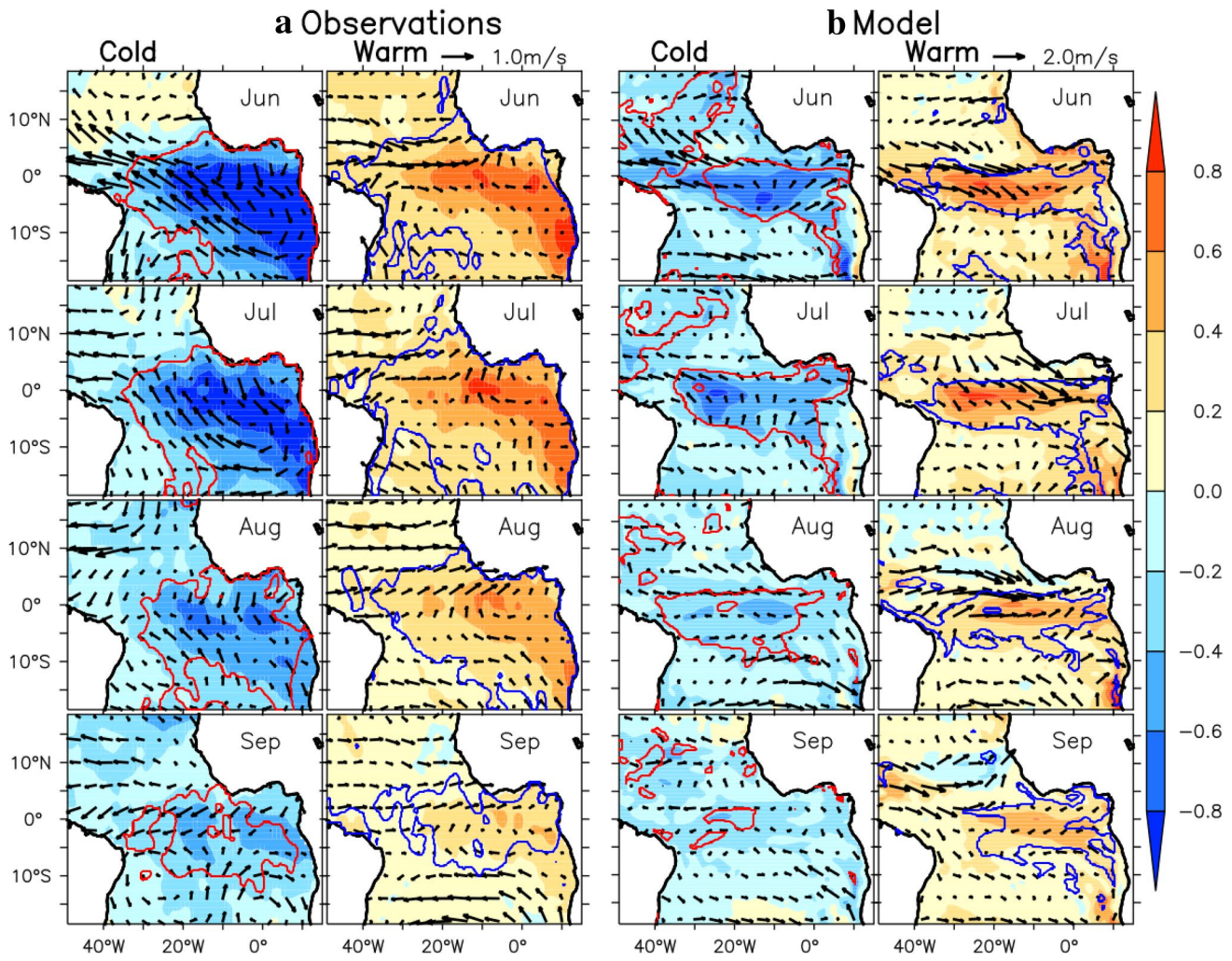

Fig. 4 Monthly composites of anomalies of SST (shaded; °C) and low level winds at 850 hPa (vectors; ms^{-1}) of cold and warm AZM events in **a** observations and **b** in the reference run ($CFSv2_{REF}$) during June–September. The red (blue) contour lines in cold (warm) composites indicate the 10% level of statistical significance

et al. 2009; Pottapinjara et al. 2014), they are in phase and are less strongly linked, in the model. It is worth noting here that this relationship between AZM and ENSO can be influenced by the mean state in the tropical Atlantic (Rodríguez-Fonseca et al.2009), and modulated by the Atlantic Meridional Overturing Circulation (AMOC; Svendsen et al. 2013) and Atlantic Multidecadal Oscillation (AMO; Martín-Rey et al. 2014). However, we will not examine the reasons for the incorrect relationship between AZM and ENSO in the model. Nonetheless, as discussed already in Sect. 2.1, this issue has been taken care of although partly, by regressing out the impact of ENSO when required in the following analyses.

The AZM operating in the tropical Atlantic influences the monsoon rainfall over remotely located Indian subcontinent during boreal summer. In Pottapinjara et al. (2014), we proposed a teleconnection mechanism by which the AZM can affect the ISM: an AZM excites a response in the mid-tropospheric temperature (TT) field, which propagates to the east and disturbs the thermal gradient between the Indian landmass and the Indian Ocean (Webster et al. 1998; Goswami and Xavier, 2005) and thereby affects the mean circulation and rainfall over India (Fig. 6a). The simulation of this teleconnection in the reference run ($CFSv2_{REF}$) is examined here. In Fig. 6, the key element of eastward propagation of TT response of the AZM is shown both for observations (Fig. 6a) and the model (Fig. 6b). In Fig. 6a, the positive correlation between the Atl3 index and the TT indicates that responding to SST and convection anomalies associated with an observed warm (cold) AZM event, the tropospheric temperature over the Atlantic and Indian Oceans rises (falls). In the observations (Fig. 6a; similar to Fig. 10 of Pottapinjara et al. 2014), the TT response in the Atlantic grows (before −1 month TT lead), peaks (between –s1 and 1 months lead)

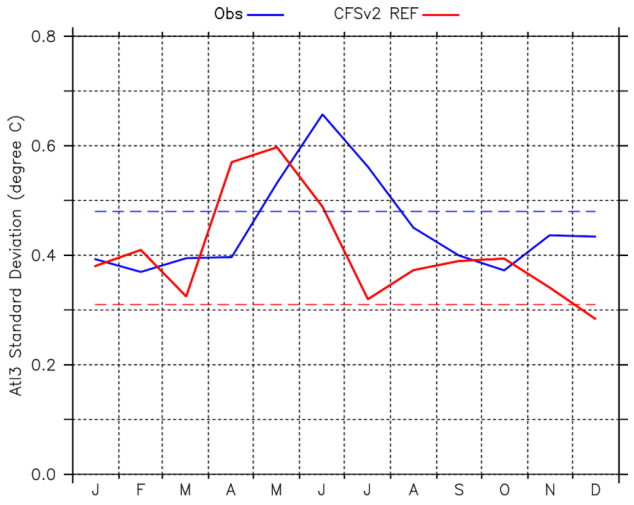

Fig. 5 Monthly standard deviations of the Atl3 index in the model reference run ($CFSv2_{REF}$; thick red line) and observations (thick blue line). The standard deviation of June–August Atl3 index is also indicated ($CFSv2_{REF}$: dashed red line; observations: dashed blue line)

and decays (after 1 month lead) with time. This Matsuno-Gill response (Matsuno 1966; Gill 1980) has a Rossby wave-like structure with two lobes of high positive correlation on either side of the equator in the Atlantic and has an eastward propagating Kelvin wave-like structure in the equatorial band (Fig. 6a). This response propagates to the east through the Indian Ocean and reaches as far as 140°E in the Pacific at its peak. The warming of the troposphere in the equatorial belt (confined between 10° S and 10° N) over the Indian Ocean can weaken the positive TT gradient between the land (Indian landmass) and ocean (Indian Ocean) that is shown to be critical for the circulation of ISM (e.g., Webster et al. 1998; Goswami and Xavier 2005). In Pottapinjara et al. (2014), the modulation of TT gradient by the AZM is argued to be intimately connected to the lower level moisture transport to the Indian subcontinent, low level cyclonic vorticity in the BoB, number of depressions in the BoB and ultimately the rainfall over central India. A similar figure (Fig. 6b) for the model tells us that an AZM in the model indeed excites a positive response in TT, similar to observations. With an exception at lags 2 and 3 in the Indian Ocean (Fig. 6b), this response is weaker overall (compare Fig. 6b with Fig. 6a) which is likely due to weaker interannual variability of the AZM SSTs in the model. It also decays faster compared to the observations. Nevertheless, the key features of the response in terms of structural similarity, propagation to the east into the Indian Ocean, and growth and decay are all captured by the model.

It is interesting to see if the simulation of the response of TT to the AZM in the model is reflected in AZM-ISMR relation as well. Figure 7 shows the correlation between the Atl3 index and precipitation over India both in observations (Fig. 7a) and in the reference run ($CFSv2_{REF}$; Fig. 7b). As reported in previous studies (e.g., Kucharski et al. 2008; Wang et al. 2009; Pottapinjara et al. 2014), the observed relationship between the AZM and ISMR is that a warm (cold) AZM decreases (increases) rainfall over the Western Ghats and central India and enhances (reduces) rainfall over northeastern India (Fig. 7a). An opposite relation between the AZM and rainfall over a band extending from the BoB to the northwest India can also be seen. However, in the model, only the relationship between the AZM and rainfall along the Western Ghats is captured correctly (Fig. 7b). Note that, in the observations, the rainfall along the Western Ghats is directly influenced by changes in the mean atmospheric circulation. On the contrary, the rainfall over central India has several contributors apart from variations of the mean flow (e.g., Pant and Kumar 1997) and for the model to capture the relation between the rainfall over central India and the AZM, all such factors need to be simulated properly. For instance, the monsoon depressions contribute to about 50% of the monsoonal rainfall over central India (Krishnamurti 1979; Yoon and Chen 2005; Krishnamurthy and Ajayamohan 2010; Praveen et al. 2015) and the AZM influences the frequency of the monsoon depressions in the BoB (Pottapinjara et al. 2014). However, due to the coarse resolution, the model may not be able to simulate the monsoon depressions and this can lead to an incorrect simulation of the relationship of AZM-rainfall over central India during summer monsoon. It is also unclear how the dry bias in the model over land plays into the AZM-ISM teleconnection over central India at intraseasonal and seasonal timescales (Narapusetty et al. 2016, 2018).

3.3 Response of the ISM to the imposed observed warm AZM SST anomaly in the sensitivity experiment

In the above, examining the model free-run ($CFSv2_{REF}$), we have shown that the model simulates the relationship between the AZM and ISMR through Kelvin wave-like features in the TT field, albeit with some shortcomings. To delineate the influence of AZM on the ISM more clearly, especially to see if the physical mechanism proposed in Pottapinjara et al. (2014) is indeed at work, a sensitivity experiment is conducted as described earlier (see Sect. 2.4 for the experiment design).

Before delving into the details of the response of ISM to the imposed warm AZM SST anomalies (Fig. 8a), the response of the model in the tropical Atlantic to the imposed anomalies needs to be discussed. A comparison of the JJA Atl3 time series from the reference ($CFSv2_{REF}$) and sensitivity ($CFSv2_{SST}$) runs is shown in Fig. 8c. The standard deviation of JJA Atl3 index based on the SSTs ultimately seen

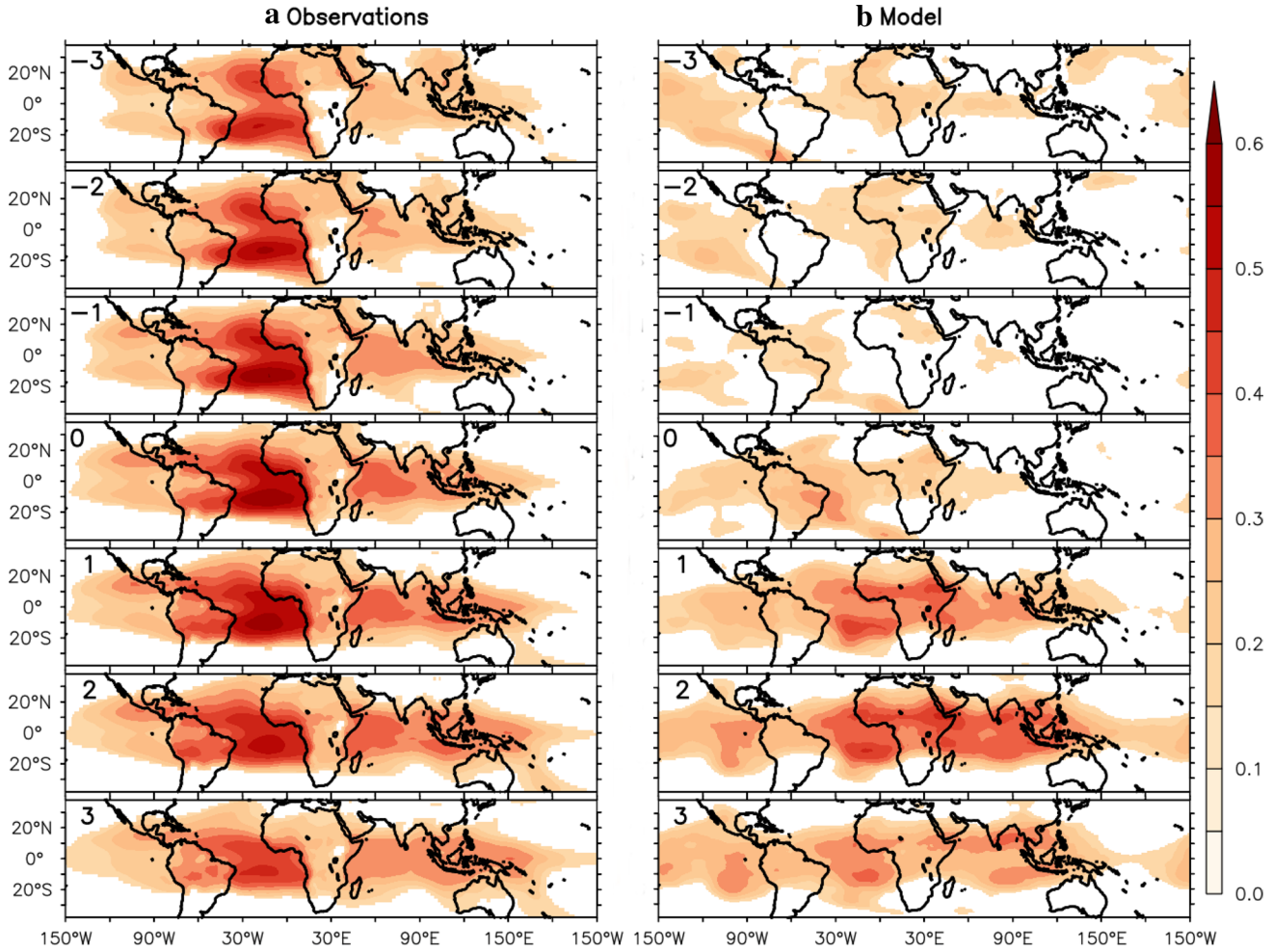

Fig. 6 Monthly lead-lag correlations between the Atl3 index and Tropospheric Temperature (TT) integrated over 600–200 hPa after removing the effect of ENSO on both TT and Atl3 index in **a** Observations and **b** Model ($CFSv2_{REF}$). The lead of TT in months is indicated on each subpanel. The effect of ENSO is removed to elicit the signal clearly. All the the correlations shown in non-white color (above 0.1) are statistically significant at the 10% level. The analysis is done covering respective full time series to keep it simple and hence, the lags do not correspond to any calendar months. Nevertheless, the signal in TT can still be seen due to the robustness of the AZM-ISM relationship

by the atmosphere in the sensitivity experiment (0.36) is slightly greater than that in the reference run (0.31) implying that the variability of the AZM in the sensitivity experiment increased only marginally. Note that the imposed AZM pattern rides on the background SSTs (directly from the oceanic component) of $CFSv2_{SST}$ which are very close to $CFSv2_{REF}$ SSTs. The addition of warm AZM SST anomaly pattern (Fig. 8a) in the tropical Atlantic in $CFSv2_{SST}$, causes warm (cold) AZM events in the $CFSv2_{REF}$ to become warmer still (near neutral) in $CFSv2_{SST}$ (Fig. 8c). Although the strength of resulting warm AZM events that are ultimately seen by the atmosphere (Fig. 8b) is a bit weaker in the southeastern tropical Atlantic (20°S–5°S and 15°W–10°E) compared to the imposed warm AZM pattern (Fig. 8a), the spatial pattern of the warm AZM in a larger region of 30°S–5°N and 30°W–10°E is very similar (compare Fig. 8b with Fig. 8a). An examination of the response of the model to warm AZM in terms of anomalies of surface wind and precipitation in the tropical Atlantic (in $CFSv2_{SST}$) tells us that the sign and magnitude of these anomalies are captured reasonably well throughout the season (figure not shown). It implies that the internal dynamics of the model do not damp away the imposed warm AZM. This gives us confidence that our sensitivity experiment achieves its goal.

The response of ISM in the model to the imposed warm AZM SST anomaly shown in Fig. 8a is discussed here (see Sect. 2.4 for details on how the model response is computed). In the subsequent analyses (Figs. 9, 10, 11, 12, 13), the difference between the $CFSv2_{SST}$ and $CFSv2_{REF}$ which is defined as the 'response' (see Sect. 2.4) to the imposed warm AZM pattern, will be used. We start with the observed relationship between AZM and ISM along

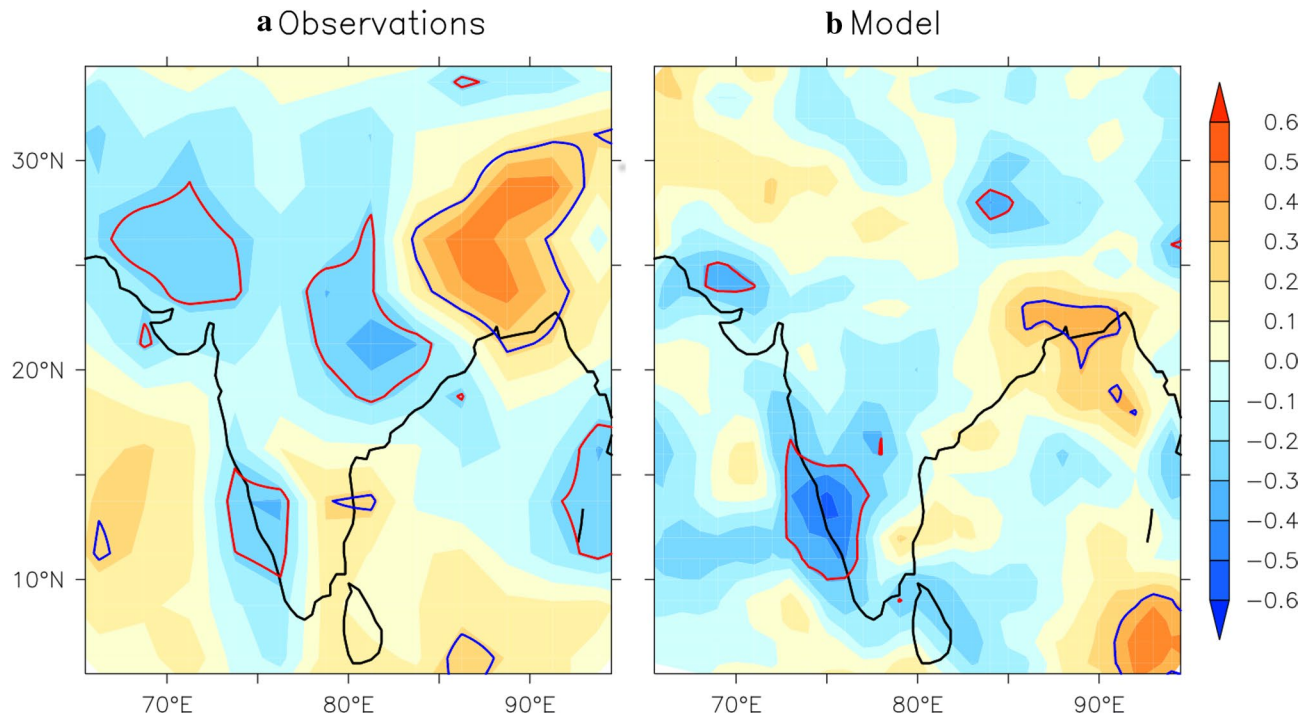

Fig. 7 The correlation between the JJA Atl3 index and the JJAS precipitation over India in **a** observations and **b** model free-run ($CFSv2_{REF}$), after removing the effect of ENSO over precipitation at each grid point. The positive (negative) correlations enclosed by blue (red) contours are significant at the 20% level

with the low level monsoonal winds in the tropical Indian Ocean shown in Fig. 9a as a reference for the analysis of the model response. In the observations, a warm AZM causes easterly wind anomalies in the eastern tropical Indian Ocean and northeasterly wind anomalies over the Arabian Sea; the net effect being a weakening of the boreal summer seasonal mean flow. As a result, a warm AZM suppresses rainfall over the Western Ghats and over a band extending from the BoB to northwest India but enhances rainfall over the eastern equatorial Indian Ocean (Fig. 9a). The seasonal (June–September) average of the response in precipitation and low level winds in the tropical Indian Ocean during summer in the model is shown in Fig. 9b. It appears that the imposition of warm SST anomaly in the tropical Atlantic weakens the low level mean flow over the Arabian Sea, in agreement with the observations, but enhances precipitation along and to the west of Western Ghats, contrary to the observations (compare with Fig. 9a). It also seems to cause an anticyclonic low level flow over central India and an increase in rainfall over the same region. The response in the low level winds in the eastern equatorial Indian Ocean is easterly, again in agreement with the observations (compare with Fig. 9a). While the model response in the low level winds is roughly as we would expect based on our earlier results in Pottapinjara et al. (2014) and the observational analysis shown in Fig. 9a, the response in the precipitation (Fig. 9b) is not consistent with the observations. More importantly, the rainfall along the Western Ghats is enhanced in response to the warm AZM SST anomaly (Fig. 9b), contrary to the observed relationship (compare with Fig. 9a). Further, the responses in the low level winds and precipitation are not consistent with each other. This apparent inconsistency must be investigated first before delving into further details.

A similar plot of monthly mean responses in precipitation and low level winds during June–September shown in Fig. 10, tells us that the two fields are consistent with each other in all individual months of the season. Whenever the response in low level winds tends to oppose (strengthen) the seasonal mean flow, precipitation is less (more) than the corresponding climatological mean. However, the response in neither the precipitation nor winds is uniform in sign throughout the season and the precipitation response is disproportionate to that of winds. For instance, the wind response of about 2 ms^{-1} along the west coast of India in September (Fig. 10d) generates disproportionately widespread and stronger precipitation response, compared to the response in precipitation accompanied by the wind response of about 4 ms^{-1} in the same region in August (Fig. 10c). Hence, the inconsistency between the wind and precipitation in the seasonal mean response shown in Fig. 9b arises from averaging their respective responses which are non-linearly related in individual months (Fig. 10). While we are focused

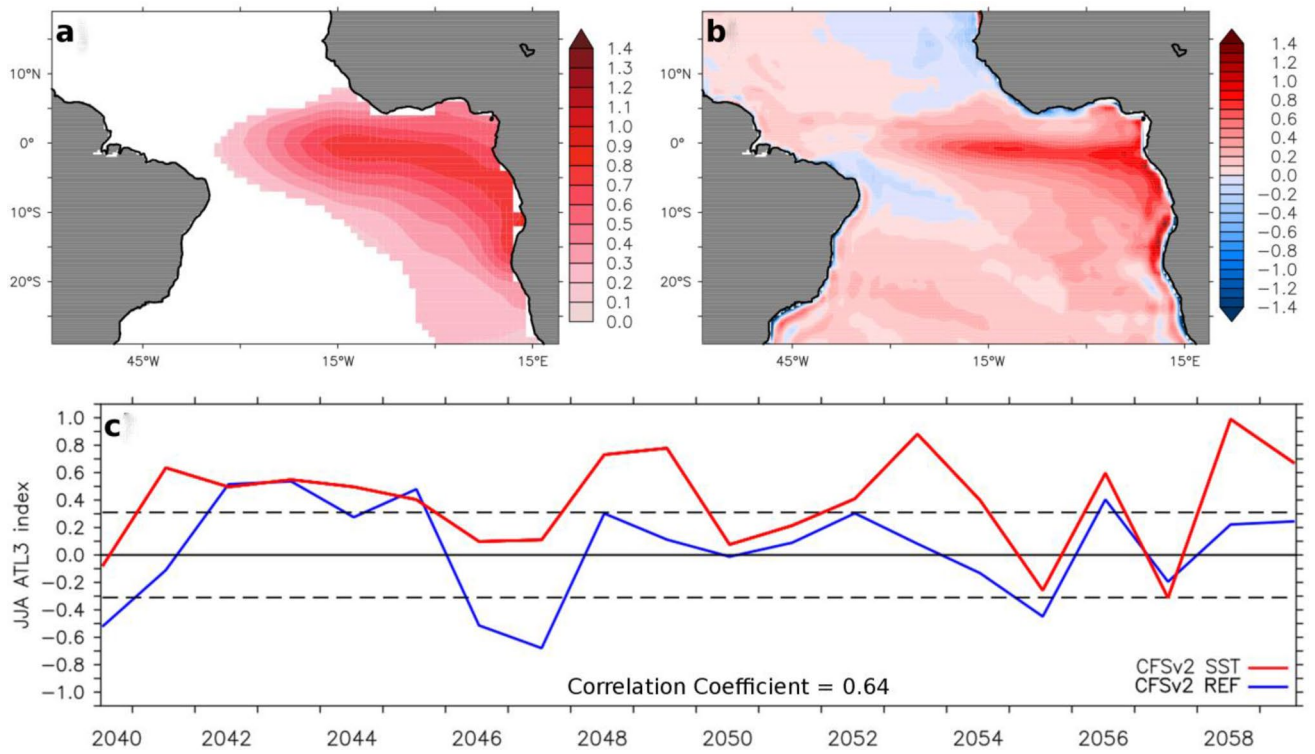

Fig. 8 Response of the model ($CFSv2_{SST}$) in the tropical Atlantic to the imposed AZM SST anomaly. **a** Composite of observed JJA SST anomalies (shaded; °C) of warm AZM events that is imposed (added at the coupler level) in the sensitivity experiment ($CFSv2_{SST}$) and **b** JJA composite of resulting warm AZM SST anomalies in $CFSv2_{SST}$, and **c** the time series of JJA Atl3 index from the reference ($CFSv2_{REF}$) and sensitivity ($CFSv2_{SST}$) runs during the common period. The composite in **a** is statistically significant at the 10% level. This same anomaly is added every year on top of the simulated tropical Atlantic SST at the coupler level in $CFSv2_{SST}$. See Sect. 2.4 for details on how this composite anomaly (**a**) is prepared. In **b**, and **c**, the SST anomalies from $CFSv2_{SST}$ used are those that are ultimately seen by the atmospheric component. In **c**, the ± 1 standard deviation of JJA Atl3 SST from the $CFSv2_{REF}$, i.e., 0.31, is indicated by black dashed lines for a comparison. When the JJA Atl3 index exceeds (falls below) the + 1 (−1) standard deviation, then a warm (cold) AZM event is considered to occur. The correlation coefficient (0.64) between the two time series is also shown

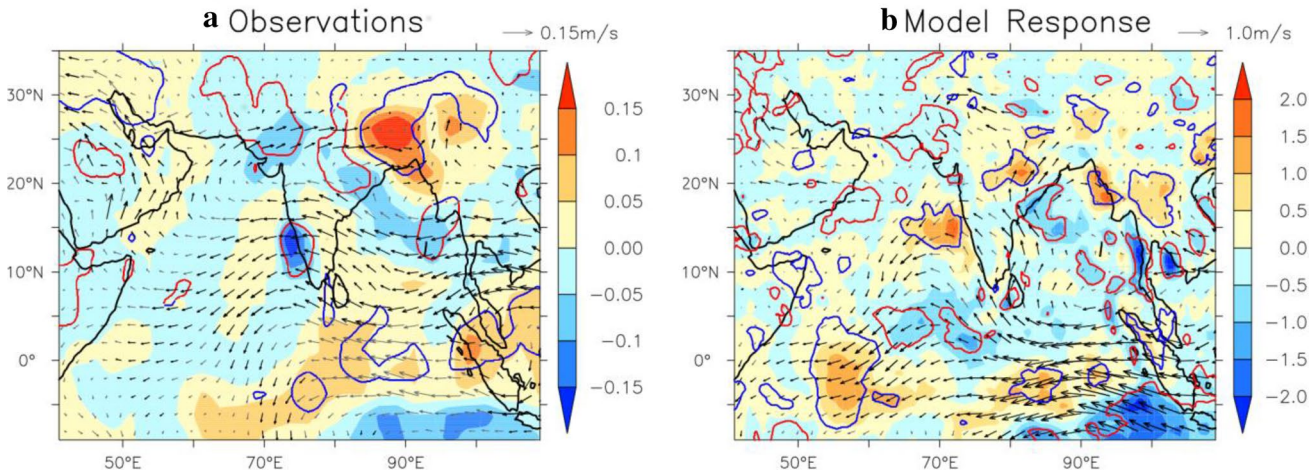

Fig. 9 Influence of AZM on the seasonal mean precipitation and low level circulation in the Indian Ocean in **a** observations and **b** model ($CFSv2_{SST}$–$CFSv2_{REF}$). **a** Regression of JJA Atl3 index onto anomalies of JJAS precipitation (shading; mm day^{-1}) and low level winds (850 hPa; vectors; ms^{-1}) after removing the influence of ENSO **b** JJAS mean model response ($CFSv2_{SST}$–$CFSv2_{REF}$) in precipitation (shading; mm day^{-1}) overlaid by winds (vectors; ms^{-1}). In **a**, the statistically significant regressions at 20% in precipitation (positive: blue; negative: red; contours) and in winds (black vectors) are marked in the aforementioned colors. In **b**, the responses in precipitation and winds statistically significant at 20% are marked similarly

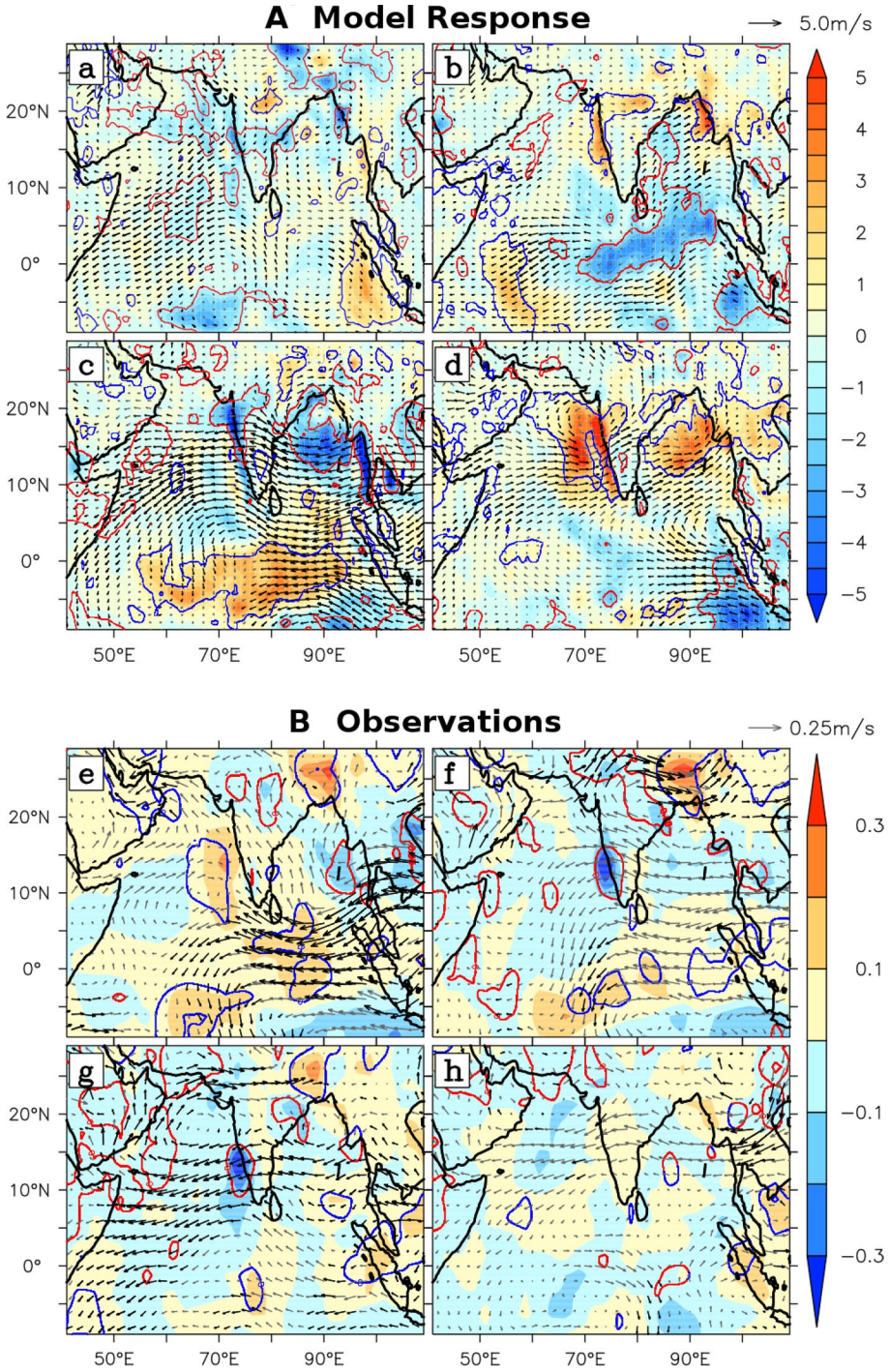

Fig. 10 **A** Model Response: Monthly mean response ($CFSv2_{SST}$–$CFSv2_{REF}$) of precipitation (shading; mm day^{-1}) overlaid by low level winds (vectors) in each month during June–September (**a** June; **b** July; **c** August; **d** September) and **B** Observations: Regression of JJA Atl3 index onto monthly anomalies of precipitation (shading; mm day^{-1}) and low level winds (850 hPa; vectors; ms^{-1}) during June–September (**e** June; **f** July; **g** August; **h** September) after removing the influence of ENSO at every grid point. In **A**, the mean responses of enhanced (reduced) precipitation and low level winds that are statically significant at the 20% level are marked in blue (red) contours and black vectors, respectively. In **B**, all parameters are taken from the respective observed datasets discussed in Sect. 2.1 and the statistically significant regressions at the 20% level in precipitation (contours; positive: blue; negative: red) and in winds (black vectors) are marked in their respective colors

on the seasonal responses here, the role of the intraseasonal variability in determining the seasonal and interannual variability may be important to consider (Goswami and Ajaya Mohan 2001). It is likely that the coastal processes and ocean control on rainfall over the west coast are an issue here as well (Xi et al. 2015). Such details need further model experiments and diagnoses but are beyond the scope of the current investigation.

In the above, we have shown that the observed relationship between AZM, and the ISMR and low level monsoonal winds in the tropical Indian Ocean (Fig. 9a) holds in the sensitivity experiment as well but only in the month of August (Fig. 10c). Further, the model response in other months is either weak (in June; Fig. 10a) or the opposite [in July (Fig. 10b) and September (Fig. 10d)]. This result is also substantiated by month-to-month comparison of the monthly ISM responses to AZM (Fig. 10a–d) during

June–September with that of observations (Fig. 10e–h; similar analysis to Fig. 9a; compare Fig. 10a with Fig. 10e and so on). Note that while Fig. 9a shows the JJAS seasonal mean influence of AZM on ISM in observations, Fig. 10e–h present a monthly evolution of the same during June–September. Focusing on the AZM-ISM relationship in August in the model (Fig. 10c), a strong easterly flow extending from the west Pacific to the Somali coast weakening the seasonal mean flow north of the equator can be observed (Figs. 10c and 12a). A strong anti-cyclonic circulation in the BoB can also be noticed (Fig. 10c). This response in winds is accompanied by a reduction in precipitation along the Western Ghats and over the BoB, and an enhancement in precipitation over the central to the eastern Indian Ocean between 10° S and 5° N. All this response is consistent with the observations (compare Fig. 10c with Fig. 9a and Fig. 10g) as well as with our earlier study (Pottapinjara et al. 2014). However, the precipitation response over central India is mixed, with a reduction over some places and an enhancement over others (Fig. 10c). As may be noted, this relation between AZM and precipitation over central India is not simulated in the model reference run ($CFSv2_{REF}$) either (Fig. 7b). Although the precipitation response along the Western Ghats in August (Fig. 10c) is consistent with the observations, the spatial extent of the precipitation response is extended further north (between 10° N and 20° N; Fig. 10c) compared to that of observations (between 10° N and 17° N; Figs. 9a and 10g). This must be related to the incorrect precipitation response over a band extending from the BoB to central India to northwest India (Fig. 10c) compared to the observations (Figs. 9a, 10g). Despite these shortcomings, on the whole, the response in the month of August (Fig. 10c) is very close to observations.

It is worth noting that the reference run ($CFSv2_{REF}$) and sensitivity experiment ($CFSv2_{SST}$) have (almost) the same mean state biases (Fig. 3). However, whereas the signals of AZM-ISM relationship can be seen in the June–September seasonal average in the reference run ($CFSv2_{REF}$; Fig. 9a), it can be seen only in August in the sensitivity experiment (Fig. 10c). It may be because the addition of SST anomalies in $CFSv2_{SST}$ is particularly more sensitive to the mean state biases in the model. To some extent, it may also be due to the simplistic design of our sensitivity experiment. Further studies are required to understand this issue, but it is beyond the scope of the present study. Before addressing the question of whether or not the response in August is consistent across different fields, we must examine why the experiment yields a response consistent with observations only in August and not in the other months of the season.

Examining the simulation of the tropical Atlantic seasonal cycle in the model may provide us a clue as to why the model response is as observed only in August. An accurate simulation of the tropical Atlantic seasonal cycle in the model is essential because the AZM is tightly phase locked to the seasonal cycle (e.g., Keenlyside and Latif 2007; Lübbecke et al. 2010; Richter et al. 2017). The meridional movement of the ITCZ is an important aspect of the tropical Atlantic seasonal cycle, and the position of the ITCZ during boreal spring is very sensitive to the contemporaneous SST gradient between the north and south tropical Atlantic, and thus links the meridional and zonal modes (Servain et al. 1999; Murtugudde et al. 2001). A comparison of climatological evolution of meridional position of the Atlantic ITCZ both in the model reference run and in the observations shows that the model simulated Atlantic ITCZ (in $CFSv2_{REF}$) is placed further away from the equator compared to the observed Atlantic ITCZ during January–April (Fig. 3). However, the ITCZ in the model (in $CFSv2_{REF}$) is located where it should be as per the observations only in the months of July–August–September and it is biased by 1.7–5 degrees latitude in January–June. The Atlantic ITCZ in the sensitivity experiment (in $CFSv2_{SST}$) coincides with that of the reference run (in $CFSv2_{REF}$) during June–September, implying that the mean state biases in the two runs remain almost the same. Therefore, with reference to boreal summer, the ITCZ seasonal cycle in the model (both $CFSv2_{REF}$ and $CFSv2_{SST}$) is delayed during boreal spring to early summer when compared to that of observations (Fig. 3). The timing of the least bias in the position of the ITCZ in the model coincides with that of the western equatorial Atlantic zonal winds (Fig. 2). As may be noted from Fig. 2, the SST bias in the southeastern tropical Atlantic also starts to decrease in August. On the other hand, in September, ISM is already withdrawing from the Indian subcontinent and for AZM to impact the ISM, ISM should also be active. Hence, only the period prior to September is likely to feel the impact of AZM on ISM. Given that the SST anomaly imposed in the tropical Atlantic in the experiment ride on the background SSTs, it may be concluded that the less-biased background conditions in the model in August both in the tropical Atlantic and the Indian Ocean, give us the desired response in the Indian Ocean region. Therefore, we will concentrate on the response in different fields in August only. Henceforth, the model response in the following would mean the response in August unless mentioned otherwise.

As mentioned earlier, AZM can influence the rainfall over central India by modulating the frequency of monsoon depressions forming in the BoB (Pottapinjara et al. 2014). As shown in Fig. 11, as a response to the imposed warm SST anomaly in the tropical Atlantic, there is a negative vorticity north of 13°N and enhanced vertical wind shear between upper and lower levels north of 17°N in the BoB, which together tend to oppose the formation of monsoon depressions in the head BoB (Pottapinjara et al. 2014). The reduced number of monsoon depressions in the BoB in turn

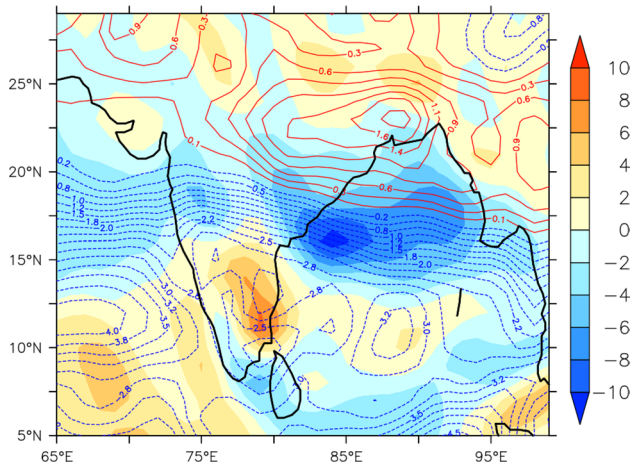

Fig. 11 The response ($CFSv2_{SST}$–$CFSv2_{REF}$) in vorticity at 850 hPa (shading; 10^{-6} s^{-1}) overlaid by magnitude of vertical wind shear between at 850 and 200 hPa (contours; shear: winds at 850 hPa—winds at 200 hPa; ms^{-1}) in August. The positive (negative) wind shear response is indicated by red (blue dashed) contours

tend to cause less rainfall over the central Indian region that is normally frequented by monsoon depressions. Although, the response in such large scale features that are critical for the monsoon depressions in the BoB are captured by the model, the rainfall response over central India is incorrect (Fig. 10c), possibly due to the low resolution of the model which is insufficient to resolve the monsoon depressions. It is also likely that the split of rainfall between the persistent and propagating modes is not accurately captured by CFSv2 as can be inferred from the dry bias related to enhanced break spells (Krishnamurthy and Shukla 2008; Narapusetty et al. 2018). Nonetheless, we can conclude that the model simulates an important result of Pottapinjara et al. (2014), at least to the extent of AZM influencing the factors affecting the formation of monsoon depressions in the BoB.

A major aspect of the teleconnection mechanism between the tropical Atlantic and Indian Oceans is through Kelvin wave-like response propagating in the tropospheric temperature field, as discussed earlier (Pottapinjara et al. 2014). To demonstrate this, the responses in different fields covering the tropical Atlantic and Indian Oceans are shown in Fig. 12. In response to the imposed warm AZM SST anomaly in the tropical Atlantic, the convection over the eastern equatorial Atlantic results in precipitation over the same region (Fig. 12b). A consistent low level westerly wind response in the central to the western equatorial Atlantic can be also noticed (Fig. 12a). In addition, as noted already, the monsoonal flow in the Indian Ocean north of the equator is weakened by the easterly wind response which extends up to 150° E (Fig. 12a; also Fig. 10c). As a result, a weak warm response in SST in the Arabian Sea can also be seen (Fig. 12c). Excited by the warm AZM SST anomaly and its resultant convection anomalies, a warm response in the mid-tropospheric temperature can be seen extending from the tropical Atlantic into the Indian Ocean and reach over to 150°E in the western Pacific (Fig. 12d). The vertical section of TT averaged over the equatorial belt covering the Atlantic and tropical Indian Oceans shown in Fig. 13a tells us that the TT in the mid-tropospheric column over the longitudes of the Atlantic indeed warms up and extends eastward into the Indian Ocean. The vertical section of the TT response in the longitudinal band of 60°E–120°E covering both the Indian subcontinent and the Indian Ocean reveals that the TT response over the Indian Ocean is warm, consistent with the warm TT response originating from the equatorial Atlantic, and it is cold over the subcontinent (Fig. 13b). This warm TT response over the ocean (Indian Ocean) and cold TT response over land (Indian subcontinent) weakens the mean land-sea mid-tropospheric thermal gradient and consequently reduces the strength of mean monsoonal flow as shown in Fig. 12a. Note that this TT response is consistent with the response in winds and precipitation shown in Fig. 12a, b, respectively, all agreeing very well with the thermodynamical aspect of the teleconnection between the AZM and ISM proposed by Pottapinjara et al. (2014).

As discussed in the Introduction, a dynamical manifestation of the response of ISM to AZM is reported by Kucharski et al. (2009). From a sensitivity experiment conducted using an AGCM, they find that a positive (negative) AZM SST anomaly in the tropical Atlantic causes a Matsuno-Gill-type baroclinic quadrupole response in the stream function. From the upper level velocity potential, they showed that the heating associated with the warm AZM event induces an upper level divergence over the tropical Atlantic and African regions, and an upper level convergence over India and the western Pacific. This is attributed to the reduction of rainfall over India. Interestingly, the upper level velocity potential in the model response presented in Fig. 12e shows a similar structure with an upper level divergence over the Atlantic and a convergence over India. In addition, the quadrupole response in lower level stream function can also be seen (Fig. 12e). Consistent with this, a reduced precipitation over India and the BoB due to the collocated upper level convergence can be also noticed (Fig. 12b). Hence, the model also simulates the dynamics-based teleconnection between the AZM and ISM proposed by Kucharski et al. (2009).

From the above discussion of results from the sensitivity experiment, we may conclude with more confidence that the observed teleconnection between the AZM and ISM is adequately captured by the model, although it misses some finer details due to mean state biases in the tropical Atlantic.

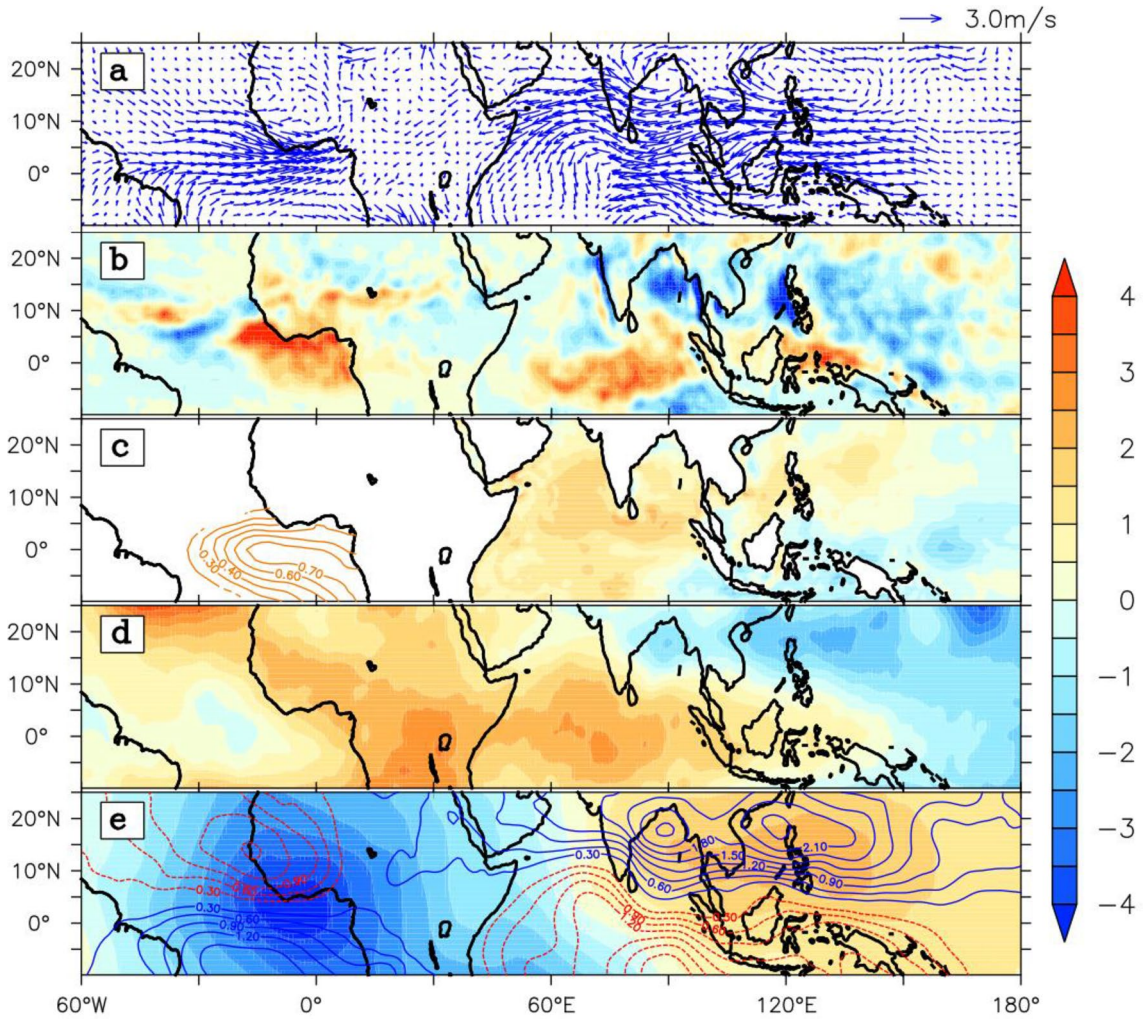

Fig. 12 The response ($CFSv2_{SST}$–$CFSv2_{REF}$) and analyses of different fields covering the tropical Atlantic and Indian Oceans in August: **a** low level wind vectors at 850 hPa (m s^{-1}), **b** precipitation (mm day^{-1}), **c** SST (°C; multiplied by 0.25), **d** mid-tropospheric temperature averaged between 600 and 200 hPa (0.1 K), and **e** upper level velocity potential at 200 hPa (shading; 10^6 m^2s^{-1}) and low level stream function at 850 hPa (contours; 10^6 m^2s^{-1}). The specified fields are scaled to have a common color scale. In **c**, the SST response in the tropical Atlantic is masked because that is where we impose the warm AZM SST anomaly shown in orange contours. In **d**, the positive (negative) contours of stream function are shown in blue (red) colors to highlight the quadrupole structure of Kucharski et al. (2009)

4 Summary and conclusion

Earlier studies have shown the existence of a relation between AZM and ISM (e.g., Kucharski et al. 2008, 2009; Wang et al. 2009; Pottapinjara et al. 2014, 2016). Importantly, in a recent study Pottapinjara et al. (2014), we have proposed a thermodynamic mechanism by which the AZM influences the ISM. In this study, we examine how well the CFSv2, a state-of-the-art ocean–atmosphere coupled model used for ISM forecasts in India, simulates the AZM-monsoon teleconnection and the physical mechanism proposed by our earlier study Pottapinjara et al (2014). The analysis of the model free-run ($CFSv2_{REF}$) suggests that variability of the AZM, AZM-monsoon relation (a warm AZM suppressing the rainfall over India), and AZM-ISM teleconnection via the mid-tropospheric temperature response affecting the land-sea thermal gradient in the Indian Ocean region are all reasonably captured in the model but are subject to the biases linked to the mean state.

We also conduct a complementary sensitivity experiment to delineate the influence of AZM on ISM. In the experiment, a warm AZM SST anomaly is imposed (added at the coupler level) in the tropical Atlantic during June–September and the response (difference between the sensitivity and reference run) of the ISM is studied. The analyses of the sensitivity experiment are analyzed in the context of the mean state biases to advance the process understanding of the AZM-monsoon interactions. Because of the delayed seasonal cycle in the tropical Atlantic

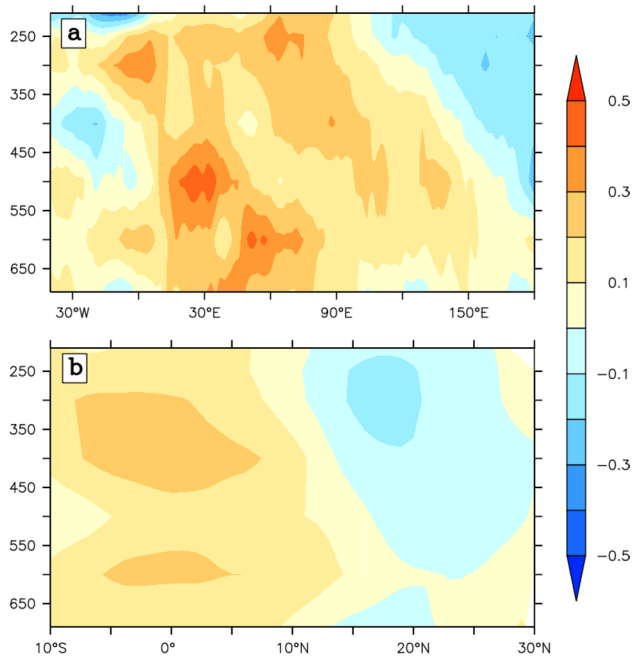

Fig. 13 Vertical cross sections of the response ($CFSv2_{SST}$–$CFSv2_{REF}$) in mid-tropospheric temperature (TT; K) in August, **a** after averaging over the latitudinal band of 5° S–5° N to show the TT teleconnection between the Atlantic and Indian Oceans and **b** after averaging over the longitudinal band of 60° E–120° E to show the gradient in TT between over the Indian subcontinent and Indian Ocean

during boreal spring to early summer in the model, the response in the precipitation and low level winds in the Indian Ocean is not consistent throughout summer. However, in the month of August, the response of ISM to imposed warm AZM SST anomaly is consistent across precipitation, low level winds, mid-tropospheric temperature, vorticity and shear; all simulating the physical mechanism suggested in Pottapinjara et al. (2014). We argue that the reason why ISM response is consistent with observations in August is because of the close-to-the-right background conditions in the tropical Atlantic in August in the model, which is reflected in the more accurate meridional position of the Atlantic ITCZ (the Atlantic ITCZ position is biased in the months prior to August). In addition, the right background conditions also exist in the Indian Ocean in August with resepct to active ISM (ISM starts to withdraw in September already). However, this attribution of the simulation of observed AZM-ISM relationship only in August to the mean state biases in the tropical Atlantic needs more support and will be explored in a future study. Examining the impact of imposed warm AZM anomaly on ISM in the model ($CFSv2_{SST}$–$CFSv2_{REF}$), we note that the reduction in rainfall along the Western Ghats is prominent as it is directly affected by the changes in the mean flow (Fig. 12b). However, the precipitation response over central India is not clearly seen owing to limitations of the model. This sensitivity experiment also shows that the model simulates the dynamics-based physical mechanism proposed by Kucharski et al. (2009) wherein a warm AZM SST anomaly generates a Matsuno-Gill-type quadrupole response and induces an upper level convergence over India leading to a reduction in ISM rainfall. The two mechanisms of Kucharski et al. (2009 and Pottapinjara et al. (2014) may not be totally independent of each other but are different manifestations of the total coupled nonlinear system.

As shown in this study, the CFSv2 model has some serious biases in simulating the seasonal cycle in the tropical Atlantic, but this problem is also seen in many coupled models participating in the CMIP5 (Richter et al. 2014; Richter 2015; Cabos et al. 2019). In this context, our study highlights the need for improving the mean state of tropical Atlantic in CFSv2 in order to account for a realistic AZM-ISM link, which will potentially lead to better forecasts of the ISM.

Although we have shown that the CFSv2 simulates the different manifestations of the response of ISM to AZM (Kucharski et al. 2009; Pottapinjara et al. 2014), we have not investigated the relative importance of these mechanisms. The responses of winds and precipitation in the Indian Ocean (Fig. 12a, b) seem a bit stronger for the imposed SST anomaly. The strong response could be due to local positive feedbacks in the Indian Ocean or a stronger dynamic response in addition to the thermodynamic response. The cooling of TT in the BoB and western Pacific (Fig. 12d) is not seen in the observations or in the $CFSv2_{REF}$ (Fig. 6). It is likely that this cooling is induced by the sinking motion over those regions as a secondary response. The enhancement of precipitation in the southeastern Indian Ocean, and reduction of precipitation over the BoB (Fig. 12b) are likely linked by the local Hadley cell in the Indian Ocean. A slight cooling of TT in the central equatorial Atlantic in Fig. 12d is due to the cooling between the levels of 400 and 350 hPa (Fig. 13a) but we do not yet understand why this occurs. In this study, while examining the simulation of the results reported in Pottapinjara et al. (2014), we did not actually track the monsoon depressions in the model as the coarse resolution of the model does not capture them. Rather, we have only shown the response in the vorticity and wind shear that are crucial for the formation of monsoon depressions in the BoB. It should be noted that in the sensitivity experiment, we have studied only the response to warm SST anomaly in the tropical Atlantic. A subsequent experiment imposing the cold SST anomaly can offer us more insights into possible non-linearity in the teleconnection between AZM and ISM with respect to the phase of AZM, which is the subject of a further study.

Acknowledgements We thank the three anonymous reviewers whose critical comments have helped us to improve the research article significantly. We acknowledge the encouragement and necessary support of Director, Indian National Centre for Ocean Information Services (INCOIS), Ministry of Earth Sciences, Government of India to carry out this work. PyFerret of PMEL, NOAA is used to generate the graphics. RM gratefully acknowledges the Visiting Faculty position at the Indian Institute of Technology, Bombay. This is INCOIS contribution number 405 and NCPOR contribution number J-120/2020-21.

Funding Indian National Centre for Ocean Information Services, Indian Institute of Tropical Meteorology, and National Centre for Polar and Ocean Research, all are supported by the Ministry of Earth Sciences, Government of India.

Availability of data and material All the observational/reanalysis data used in this work are publicly available and the data sources are indicated clearly in the text.

Code availability The code of the coupled model used in this study, i.e., the NCEP Climate Forecast System version 2, is available at https://cfs.ncep.noaa.gov/cfsv2/downloads.html.

Declarations

Conflicts of interest The authors declare no conflicts of interest.

References

Adler RF et al (2003) The version-2 global precipitation climatology project (gpcp) monthly precipitation analysis (1979–present). J Hydrometerol 4:1147–1167. https://doi.org/10.1175/1525-7541(2003)004%3c1147:TVGPCP%3e2.0.CO;2

Amat HB, Ashok K (2018) Relevance of Indian summer monsoon and its tropical Indo-Pacific climate drivers for the Kharif crop production. Pure and Appl Geophys 175(6):2307–2322. https://doi.org/10.1007/s00024-017-1758-9

Ashok K, Guan Z, Yamagata T (2001) Impact of the Indian Ocean dipole on the relationship between the Indian monsoon rainfall and ENSO. Geophys Res Lett 28(33):4499–5502. https://doi.org/10.1029/2001GL013294

Ashok K, Feba F, Tejavath CT (2019) The Indian summer monsoon rainfall and ENSO. Mausam 70(3):443–452

Barimalala R, Bracco A, Kucharski F, McCreary JP, Crise A (2013) Arabian Sea ecosystem responses to the South Tropical Atlantic teleconnection. J Mar Syst 117:14–30. https://doi.org/10.1016/j.jmarsys.2013.03.002

Behera S, Krishnan R, Yamagata T (1999) Unusual ocean-atmosphere conditions in the tropical Indian Ocean during 1994. Geophy Res Lett 26(19):3001–3004. https://doi.org/10.1029/1999GL010434

Burls N, Reason CC, Penven P, Philander S (2012) Energetics of the tropical Atlantic zonal mode. J Clim 25(21):7442–7466. https://doi.org/10.1175/JCLI-D-11-00602.1

Cabos W, de la Vara A, Koseki S (2019) Tropical Atlantic variability: observations and modeling. Atmosphere 10:502. https://doi.org/10.3390/atmos10090502

Colas F, McWilliams J, Capet X, Kurian J (2012) Heat balance and eddies in the Peru-Chile current system. Clim Dyn 39:509–529. https://doi.org/10.1007/s00382-011-1170-6

Dee DP et al (2011) The ERA-Interim reanalysis: configuration and performance of the data assimilation system. Q J R Meteorol Soc 137(656):553–597. https://doi.org/10.1002/qj.828

Dippe T, Krebs M, Harlaß J, Lübbecke JF (2018) Can climate models simulate the observed strong summer surface cooling in the equatorial Atlantic? YOUMARES 8–Oceans across boundaries: learning from each other, vol 7–23. Springer, Berlin. https://doi.org/10.1007/978-3-319-93284-2_2

Gadgil S (2018) The monsoon system: land–sea breeze or the ITCZ? J Earth Syst Sci. https://doi.org/10.1007/s12040-017-0916-x

Gadgil S, Gadgil S (2006) The Indian monsoon, GDP and agriculture. Econ Political Wkly 41:4887–4895

Gadgil S, Sajani S (1998) Monsoon precipitation in the AMIP runs. Clim Dyn 14:659–689. https://doi.org/10.1007/s003820050248

George G, Rao DN, Sabeerali C, Srivastava A, Rao SA (2016) Indian summer monsoon prediction and simulation in CFSv2 coupled model. Atmos Sci Lett 17(1):57–64. https://doi.org/10.1002/asl.599

Gill AE (1980) Some simple solutions for heat-induced tropical circulation. Q J Royal Meteorol Soc 106(449):447–462. https://doi.org/10.1002/qj.49710644905

Goswami BN, Ajaya Mohan RS (2001) Intraseasonal oscillations and interannual variability of the Indian summer monsoon. J Clim 14(6):1180–1198. https://doi.org/10.1175/1520-0442(2001)014%3c1180:IOAIVO%3e2.0.CO;2

Goswami B, Xavier PK (2005) ENSO control on the south Asian monsoon through the length of the rainy season. Geophy Res Lett. https://doi.org/10.1029/2005GL023216

Goubanova K, Sanchez-Gomez E, Frauen C, Voldoire A (2019) Respective roles of remote and local wind stress forcings in the development of warm SST errors in the South-Eastern Tropical Atlantic in a coupled high-resolution model. Clim Dyn 52:1359–1382. https://doi.org/10.1007/s00382-018-4197-0

Harlaß J, Latif M, Park W (2018) Alleviating tropical Atlantic sector biases in the Kiel climate model by enhancing horizontal and vertical resolution: Climatology and interannual variability. Clim Dyn 50:2605–2635. https://doi.org/10.1007/s00382-017-3760-4

Jansen M, Dommenget D, Keenlyside N (2009) Tropical atmosphere–ocean interactions in a conceptual framework. J Clim 22(3):550–567. https://doi.org/10.1175/2008JCLI2243.1

Jiang X, Yang S, Li Y, Kumar A, Liu X, Zuo Z, Jha B (2013) Seasonal-to-interannual prediction of the Asian summer monsoon in the NCEP Climate Forecast System version 2. J Clim 26(11):3708–3727. https://doi.org/10.1175/JCLI-D-12-00437.1

Keenlyside NS, Latif M (2007) Understanding equatorial Atlantic interannual variability. J Clim 20(1):131–142. https://doi.org/10.1175/JCLI3992.1

Keshavamurty RN (1982) Response of the atmosphere to sea surface temperature anomalies over the equatorial Pacific and the teleconnections of the Southern Oscillation. J Atmos Sci 39(6):1241–1259. https://doi.org/10.1175/1520-0469(1982)039%3c1241:ROTATS%3e2.0.CO;2

Kothawale D, Rajeevan M (2017) Monthly, seasonal and annual rainfall time series for all-India, homogeneous regions and meteorological subdivisions: 1871–2016. IITM Research Report No. RR-138, ISSN 0252-1075

Krishnamurthy V (2018) Seasonal prediction of South Asian monsoon in CFSv2. Clim Dyn 51:1427–1448. https://doi.org/10.1007/s00382-017-3963-8

Krishnamurthy V, Ajayamohan R (2010) Composite structure of monsoon low pressure systems and its relation to Indian rainfall. J Clim 23(16):4285–4305. https://doi.org/10.1175/2010JCLI2953.1

Krishnamurthy V, Shukla J (2000) Intraseasonal and interannual variability of rainfall over India. J Clim 13(24):4366–4377. https://doi.org/10.1175/1520-0442(2000)013%3c0001:IAIVOR%3e2.0.CO;2

Krishnamurthy V, Shukla J (2008) Seasonal persistence and propagation of intraseasonal patterns over the Indian monsoon region. Clim Dyn 30:353–369. https://doi.org/10.1007/s00382-007-0300-7

Krishnamurti TN (1979) Tropical meteorology, In: Wiin-Nielsen A (ed) Compendium of meteorology II, WMO-No. 364, World Meteorological Organization, Geneva, Switzerland

Kucharski F, Bracco A, Yoo J, Molteni F (2007) Low-frequency variability of the Indian monsoon–ENSO relationship and the tropical Atlantic: the weakening of the 1980s and 1990s. J Clim 20(16):4255–4266. https://doi.org/10.1175/JCLI4254.1

Kucharski F, Bracco A, Yoo J, Molteni F (2008) Atlantic forced component of the Indian monsoon interannual variability. Geophys Res Lett. https://doi.org/10.1029/2007GL033037

Kucharski F, Bracco A, Yoo J, Tompkins A, Feudale L, Ruti P, Dell'Aquila A (2009) A Gill–Matsuno-type mechanism explains the tropical Atlantic influence on African and Indian monsoon rainfall. Q J R Meteorol Soc 135(640):569–579. https://doi.org/10.1002/qj.406

Kucharski F et al (2016) The teleconnection of the tropical Atlantic to Indo-Pacific sea surface temperatures on inter-annual to centennial time scales: a review of recent findings. Atmosphere 7(2):29. https://doi.org/10.3390/atmos7020029

Kumar A, Pai D, Singh J, Singh R, Sikka D (2012) Statistical models for long-range forecasting of southwest monsoon rainfall over India using step wise regression and neural network. Atmos Clim Sci 2(03):322. https://doi.org/10.4236/acs.2012.23029

Large WG, Danabasoglu G (2006) Attribution and impacts of upper-ocean biases in CCSM3. J Clim 19(11):2325–2346. https://doi.org/10.1175/JCLI3740.1

Lübbecke JF, McPhaden MJ (2013) A comparative stability analysis of Atlantic and Pacific Niño modes. J Clim 26(16):5965–5980. https://doi.org/10.1175/JCLI-D-12-00758.1

Lübbecke JF, Rodríguez-Fonseca B, Richter I, Martín-Rey M, Losada T, Polo I, Keenlyside NS (2018) Equatorial Atlantic variability: Modes, mechanisms, and global teleconnections. Wiley Interdiscip Rev Clim Change 9(4):e527. https://doi.org/10.1002/wcc.527

Lübbecke JF, Böning CW, Keenlyside NS, Xie S-P (2010) On the connection between Benguela and equatorial Atlantic Niños and the role of the South Atlantic Anticyclone. J Geophys Res Oceans. https://doi.org/10.1029/2009JC005964

Marchesiello P, McWilliams J, Schepetkin A (2003) Equilibrium structure and dynamics of the californian current system. J Phys Oceanogr 33(4):753–783. https://doi.org/10.1175/1520-0485(2003)33%3c753:ESADOT%3e2.0.CO;2

Martín-Rey M, Rodríguez-Fonseca B, Polo I, Kucharski F (2014) On the Atlantic–Pacific Niños connection: a multidecadal modulated mode. Clim Dyn 43:3163–3178

Matsuno T (1966) Quasi-geostrophic motions in the equatorial area. J Meteorol Soc Japan Ser II 44(1):25–43. https://doi.org/10.2151/jmsj1965.44.1_25

Mooley D, Parthasarathy B (1984) Indian summer monsoon and the east equatorial Pacific sea surface temperature. Atmos Ocean 22(1):23–35. https://doi.org/10.1080/07055900.1984.9649182

Murtugudde R, McCreary JP Jr, Busalacchi AJ (2000) Oceanic processes associated with anomalous events in the Indian Ocean with relevance to 1997–1998. J Geophys Res Oceans 105(C2):3295–3306. https://doi.org/10.1029/1999JC900294

Murtugudde RG, Ballabrera-Poy J, Beauchamp J, Busalacchi AJ (2001) Relationship between zonal and meridional modes in the tropical Atlantic. Geophys Res Lett 28(23):4463–4466. https://doi.org/10.1029/2001GL013407

Narapusetty B, Murtugudde R, Wang H, Kumar A (2016) Ocean–atmosphere processes driving Indian summer monsoon biases in CFSv2 hindcasts. Clim Dyn 47(5–6):1417–1433. https://doi.org/10.1007/s00382-015-2910-9

Narapusetty B, Murtugudde R, Wang H, Kumar A (2018) Ocean–atmosphere processes associated with enhanced Indian monsoon break spells in CFSv2 forecasts. Clim Dyn 51(7–8):2623–2636. https://doi.org/10.1007/s00382-017-4032-z

Pai D, Sreejith O, Nargund S, Musale M, Tyagi A (2011) Present operational long range forecasting system for southwest monsoon rainfall over India and its performance during 2010. Mausam 62(2):179–196

Pai D, Rao AS, Senroy S, Pradhan M, Pillai PA, Rajeevan M (2017) Performance of the operational and experimental long-range forecasts for the 2015 southwest monsoon rainfall. Curr Sci 112:68–75

Pai D, Rao AS, Sreejith O, Bandgar A, Surendran D (2019) Forecasting the Monsoon. Geogr You 19(8):10–15

Pant GB, Kumar KR (1997) Climates of south Asia. Wiley, Hoboken. https://doi.org/10.1002/(SICI)1097-0088(199804)18:5<581::AID-JOC267>3.0.CO;2-%23

Parthasarathy B, Munot A, Kothawale D (1994) All-India monthly and seasonal rainfall series: 1871–1993. Theor Appl Climatol 49(4):217–224. https://doi.org/10.1007/BF00867461

Pattanaik D et al (2019) Evolution of operational extended range forecast system of IMD: prospects of its applications in different sectors. Mausam 7(2):233–264

Philander SG (1989) El Niño, La Niña, and the southern oscillation. In: International geophysics series, vol 46. Academic Press, Cambridge, USA, p 10-289

Pottapinjara V, Girishkumar MS, Ravichandran M, Murtugudde R (2014) Influence of the Atlantic zonal mode on monsoon depressions in the Bay of Bengal during boreal summer. J Geophys Res Atmos 119(11):6456–6469. https://doi.org/10.1002/2014JD021494

Pottapinjara V, Girishkumar MS, Sivareddy S, Ravichandran M, Murtugudde R (2016) Relation between the upper ocean heat content in the equatorial Atlantic during boreal spring and the Indian monsoon rainfall during June–Spetember. Int J Climatol 36:2469–2480. https://doi.org/10.1002/joc.4506

Pottapinjara V, Girishkumar MS, Murtugudde R, Ashok K, Ravichandran M (2019) On the relation between the boreal spring position of the Atlantic intertropical convergence zone and Atlantic zonal mode. J Clim 32(15):4767–4781. https://doi.org/10.1175/JCLI-D-18-0614.1

Pottapinjara V (2020) A study on links between the tropical Atlantic and Indian summer monsoon on interannual timescales. PhD Thesis, University of Hyderabad

Praveen V, Sandeep S, Ajayamohan R (2015) On the relationship between mean monsoon precipitation and low pressure systems in climate model simulations. J Clim 28(13):5305–5324. https://doi.org/10.1175/JCLI-D-14-00415.1

Ramu DA et al (2016) Indian summer monsoon rainfall simulation and prediction skill in the CFSv2 coupled model: Impact of atmospheric horizontal resolution. J Geophys Res Atmos 121(5):2205–2221. https://doi.org/10.1002/2015JD024629

Rao SA et al (2019) Monsoon mission: a targeted activity to improve monsoon prediction across scales. Bull Am Meteorol Soc 100(12):2509–2532. https://doi.org/10.1175/BAMS-D-17-0330.1

Rasmusson EM, Carpenter TH (1982) Variations in tropical sea surface temperature and surface wind fields associated with the Southern Oscillation/El Niño. Mon Weather Rev 110(5):354–384. https://doi.org/10.1175/1520-0493(1982)110%3c0354:VITSST%3e2.0.CO;2

Rayner N, Parker DE, Horton E, Folland CK, Alexander LV, Rowell D, Kent E, Kaplan A (2003) Global analyses of sea surface temperature, sea ice, and night marine air temperature since the late nineteenth century. J Geophys Res Atmos. https://doi.org/10.1029/2002JD002670

Richter I (2015) Climate model biases in the eastern tropical oceans: causes, impacts and ways forward. WIREs Climate Change 3(6):345–358. https://doi.org/10.1002/wcc.338

Richter I, Tokinaga H (2020) An overview of the performance of CMIP6 models in the tropical Atlantic: mean state, variability, and remote impacts. Clim Dyn 55:2579–2601. https://doi.org/10.1007/s00382-020-05409-w

Richter I, Xie S-P, Behera SK, Doi T, Masumoto Y (2014) Equatorial Atlantic variability and its relation to mean state biases in CMIP5. Clim Dyn 42(1–2):171–188. https://doi.org/10.1007/s00382-012-1624-5

Richter I, Xie S-P, Morioka Y, Doi T, Taguchi B, Behera S (2017) Phase locking of equatorial Atlantic variability through the seasonal migration of the ITCZ. Clim Dyn 48(11–12):3615–3629. https://doi.org/10.1007/s00382-016-3289-y

Rodríguez-Fonseca B, Polo I, García-Serrano J, Losada T, Mohino E, Mechoso CR, Kucharski F (2009) Are Atlantic Niños enhancing Pacific ENSO events in recent decades? Geophys Res Lett 36:L20705

Roxy M, Tanimoto Y, Preethi B, Terray P, Krishnan R (2013) Intraseasonal SST-precipitation relationship and its spatial variability over the tropical summer monsoon region. Clim Dyn 41:45–61. https://doi.org/10.1007/s00382-012-1547-1

Roxy MK, Ritika K, Terray P, Murtugudde R, Ashok K, Goswami B (2015) Drying of Indian subcontinent by rapid Indian Ocean warming and a weakening land-sea thermal gradient. Nat Commun 6:7423. https://doi.org/10.1038/ncomms8423

Ruiz-Barradas A, Carton JA, Nigam S (2000) Structure of interannual-to-decadal climate variability in the tropical Atlantic sector. J Clim 13(18):3285–3297. https://doi.org/10.1175/1520-0442(2000)013%3c3285:SOITDC%3e2.0.CO;2

Sabeerali C, Ajayamohan R, Bangalath HK, Chen N (2019a) Atlantic zonal mode: an emerging source of indian summer monsoon variability in a warming world. Geophys Res Lett 46(8):4460–4467. https://doi.org/10.1029/2019GL082379

Sabeerali C, Ajayamohan R, Rao SA (2019b) Loss of predictive skill of Indian summer monsoon rainfall in NCEP CFSv2 due to misrepresentation of Atlantic zonal mode. Clim Dyn 52(7–8):4599–4619. https://doi.org/10.1007/s00382-018-4390-1

Saha S et al (2014a) The NCEP climate forecast system version 2. J Clim 27(6):2185–2208. https://doi.org/10.1175/JCLI-D-12-00823.1

Saha SK et al (2014b) Improved simulation of Indian summer monsoon in latest NCEP climate forecast system free run. Int J Climatol 34(5):1628–1641. https://doi.org/10.1002/joc.3791

Saha SK et al (2016) Potential predictability of Indian summer monsoon rainfall in NCEP CFSv2. J Adv Model Earth Syst 8(1):96–120. https://doi.org/10.1002/2015MS000542

Sahai A, Chattopadhyay R, Joseph S, Krishna PM, Pattanaik D, Abhilash S (2019) Seamless Prediction of Monsoon Onset and Active/Break Phases. In: Robert A, Vitart F (eds) Sub-seasonal to seasonal prediction. Elsevier, Amsterdam, pp 421–438. doi: https://doi.org/10.1016/B978-0-12-811714-9.00020-6

Sahana AS, Pathak A, Roxy MK, Ghosh S (2019) Understanding the role of moisture transport on the dry bias in Indian monsoon simulations by CFSv2. Clim Dyn 52(1–2):637–651. https://doi.org/10.1007/s00382-018-4154-y

Saji N, Goswami B, Vinayachandran P, Yamagata T (1999) A dipole mode in the tropical Indian Ocean. Nature 401(6751):360. https://doi.org/10.1038/43854

Servain J, Wainer I, McCreary JP Jr, Dessier A (1999) Relationship between the equatorial and meridional modes of climatic variability in the tropical Atlantic. Geophys Res Lett 26(4):485–488. https://doi.org/10.1029/1999GL900014

Servain J, Wainer I, Ayina HL, Roquet H (2000) The relationship between the simulated climatic variability modes of the tropical Atlantic. Int J Climatol 20(9):939–953. https://doi.org/10.1002/1097-0088(200007)20:9%3c939::AID-JOC511%3e3.0.CO;2-V

Shukla RP, Huang B (2016) Mean state and interannual variability of the Indian summer monsoon simulation by NCEP CFSv2. Clim Dyn 46:3845–3864. https://doi.org/10.1007/s00382-015-2808-6

Sikka D (1980) Some aspects of the large scale fluctuations of summer monsoon rainfall over India in relation to fluctuations in the planetary and regional scale circulation parameters. Proc Ind Acad Sci-Earth Planet Sci 89(2):179–195. https://doi.org/10.1007/BF02913749

Svendsen L, Kvamstø N, Keenlyside N (2013) Weakening AMOC connects Equatorial Atlantic and Pacific interannual variability. Clim Dyn 43:2931–2941

Wang C, Kucharski F, Barimalala R, Bracco A (2009) Teleconnections of the tropical Atlantic to the tropical Indian and Pacific Oceans: a review of recent findings. Meteorol Z 18(4):445–454. https://doi.org/10.1127/0941-2948/2009/0394

Webster PJ, Magana VO, Palmer T, Shukla J, Tomas R, Yanai M, Yasunari T (1998) Monsoons: processes, predictability, and the prospects for prediction. J Geophys Res: Oceans 103(C7):14451–14510. https://doi.org/10.1029/97JC02719

Webster PJ, Moore AM, Loschnigg JP, Leben RR (1999) Coupled ocean–atmosphere dynamics in the Indian Ocean during 1997–98. Nature 401(6751):356. https://doi.org/10.1038/43848

Xi J, Zhou L, Murtugudde R, Jiang L (2015) Impacts of intraseasonal SST anomalies on precipitation during indian summer monsoon. J Clim 28(11):4561–4575. https://doi.org/10.1175/JCLI-D-14-00096.1

Xie S-P, Carton JA (2004) Tropical Atlantic variability: Patterns, mechanisms, and impacts. In: Wang C, Xie SP, Carton SP (eds) Earth climate: the ocean–atmosphere interaction, vol 147. Washington, D.C., USA, pp 121–142. https://doi.org/10.1029/147GM07

Xu Z, Chang P, Richter I, Kim W, Tang G (2014) Diagnosing the southeast tropical Atlantic SST and ocean circulation biases in the CMIP5 ensemble. Clim Dyn 43:3123–3145. https://doi.org/10.1007/s00382-014-2247-9

Yadav RK, Srinivas G, Chowdary JS (2018) Atlantic Niño modulation of the Indian summer monsoon through Asian jet. Npj Climate and Atmospheric Science 1(1):23. https://doi.org/10.1038/s41612-018-0029-5

Yoon J-H, Chen TC (2005) Water vapor budget of the Indian monsoon depression. Tellus A 57(5):770–782. https://doi.org/10.1111/j.1600-0870.2005.00145.x

Zebiak SE (1993) Air–sea interaction in the equatorial Atlantic region. J Clim 6(8):1567–1586. https://doi.org/10.1175/1520-0442(1993)006%3c1567:AIITEA%3e2.0.CO;2

Zuidema P (2016) Challenges and prospects for reducing coupled climate model SST biases in the eastern tropical Atlantic and Pacific oceans: The US CLIVAR Eastern Tropical Oceans synthesis working group. Bull A Meteorol Soc 97(12):2305–2328. https://doi.org/10.1175/BAMS-D-15-00274.1